NUMERICAL STUDY OF INCOMPRESSIBLE FLUID FLOW IN A VERTICALLY DROPPING POOL WITH AND WITHOUT END SILL

by

VIMAL RAMANUJ

Presented to the Faculty of the Graduate School of
The University of Texas at Arlington in Partial Fulfillment
of the Requirements
for the Degree of

MASTER OF SCIENCE IN MECHANICAL ENGINEERING

THE UNIVERSITY OF TEXAS AT ARLINGTON

August 2013

Acknowledgements

I would like to thank my supervising professor Dr. Albert Y. Tong for his support in the research and my academic career. He has motivated me to work to the best of my potential. Moreover, the technical input from Dr. Lin at The National Chung Hsing University, Taiwan, proved to be very helpful in my research which I highly appreciate. I would also like to thank Dr. Ratan Kumar and Dr. Luca Massa for being on the committee and their time in reviewing this project. I also appreciate the support of my colleagues Yin Guan and Peter Martinez.

Moreover, I am grateful to the Mechanical and Aerospace Engineering Department at UT Arlington for the financial and technical support that I received during the course of this research. In the end, I must mention that the moral support from my family has enabled me to pursue and excel in the field of my interest.

June 10, 2013

Abstract

NUMERICAL STUDY OF INCOMPRESSIBLE FLUID FLOW

IN A VERTICALLY DROPPING POOL

WITH AND WITHOUT END SILL

Vimal Ramanuj, M.S.

The University of Texas at Arlington, 2013

Supervising Professor: Albert Y. Tong

The study involves numerical analysis of flow field for three different flow regimes taking place in a vertically dropping pool. In general, a vertically dropping flow generates a skimming flow regime with one recirculation zone along with a developing shear layer. The presence of an obstacle (end sill) results in the formation of another recirculation zone downstream of the impinging jet. Based on the nature of these zones, the flow is categorized as napped, periodically oscillatory and skimming. The type of flow regime depends on the flow parameters like velocity and depth of flow which are controlled by Froude number. Unlike a skimming flow, shear layer in a napped flow is under the influence of two opposite circulations which affect the velocity profile in this region. The recirculation zones in case of an oscillatory flow keep changing periodically. Hence, the velocity profiles would be similar to those of napped and skimming patterns alternatively in one period. The effect of end sill and flow parameters on flow regimes has been studied. Velocity profiles within the shear layer and recirculation zones are examined and found to be in agreement with experimental findings reported in literature.

The governing equations for the flow are solved by a finite volume scheme with a two-step projection method on a fixed computational domain. The free surface is tracked using a coupled level set and volume-of-fluid method with a piecewise linear interface construction scheme.

Table of Contents

List of Illustrations

List of Tables

Chapter 1

Introduction

1.1 Overview

Open channel hydraulics has remained an important field of research within Mechanical and Civil Engineering. Civil structures like dams, spillways, energy dissipators, overfalls etc. are a few of the many areas where open channel hydraulics and fluid mechanics play an important role. Since the early 20th century, various experimental and analytical studies have been taking place in this field [1]. Experimental research in open channel hydraulics interested quite a few engineers during 1960's and 70'. Though the idea of dams and canals has been in existence since ancient times, its efficient design and application for flood prevention, energy dissipators and aerators came into existence in the 20th century. Recently, research in hydro-electricity has been made possible by the application of hydraulics and fluid science. Hydro-electricity is one of the most promising areas of research and application. Yet, most of the research work in open channel hydraulics has remained experimental to a large extent.

With the evolution and development of computational power in the late 20th century, numerical and computational techniques in design and analysis became possible and proved to be very useful in almost all engineering applications. Numerical techniques have been widely used in fields like aerodynamics and aerospace applications, structural analysis, thermal science and fluid dynamics etc. But there are still some areas which have not been exposed to numerical and computational techniques. Open Channel Hydraulics remains one of those. Numerical and computational methods save valuable resources like time and energy. But there are certain limitations associated with it too. Accuracy, reliability and consistency of the results pose a huge challenge in any numerical analysis. Failure of certain methods to

demonstrate real life situations may sometimes lead to devastating consequences. Hence, validation of a numerical study with experimental outcomes is always vital in any situation. This is why numerical studies have a great scope of further research and development.

The present study deals with flow in a vertically dropping pool which is one of the many applications of open channel hydraulics and fluid dynamics. It is worth emphasizing here that such a study is quite different from the study of a backward facing step in a flow. Backward facing step is an example of shallow water waves in which the governing equations can be approximated to simplify the solutions. While flow over a vertical drop falls under hydraulics and open channel flows. Flow over a vertical drop finds application in areas like dam constructions, canal designs, spillways, energy dissipators etc. Fluid flow over a vertically dropping pool has some critical properties associated with it, which, if not taken into consideration could lead to unexpected situations. This particular study is intended to numerically model and analyze a flow over a vertically dropping pool with and without the presence of end sill. The main objective of the study is to numerically obtain the flow field in such a situation. Knowing the flow field enables one to perform a wide range of analysis. The primary focus of the study is the classification of flow regimes as proposed in [2] and the effect of an obstacle i.e. end sill on these flow regimes. In general flow over a vertical fall without end sill results in a skimming flow regime. But the presence of an 'end sill' may result into three different flow regimes depending on certain flow properties. These are napped flow, periodically oscillatory flow and skimming flow as shown in Figure 1-1. Detailed discussion about these regimes is presented in subsequent chapters. Based on the numerical results obtained, the velocity profiles and recirculation zones are also studied and compared with the experimental findings reported in [2,3,4].

Moreover, the velocity profile within the shear layer is also presented for different types of flows. In the end, a brief description about certain applications of this study is presented.

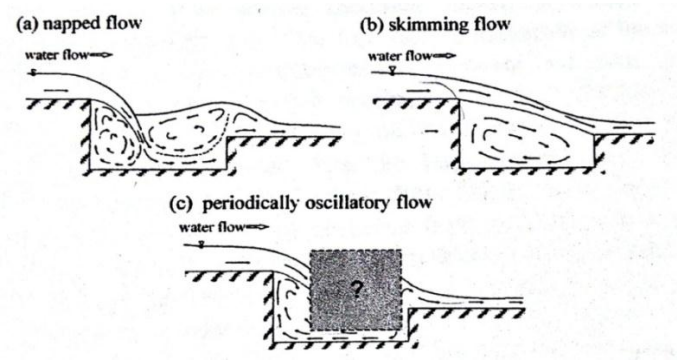

Figure1-1 Flow regimes in a vertically dropping pool with end sill [2]

1.2 Literature Review

Flow of a fluid over a vertical fall has been studied since long by researchers in the field of hydraulics and open channel flows. Hydraulics in general is studied assuming the flow to be incompressible. These studies are used in open channel structures like dams, spillways and stepped cascades to dissipate the energy of the approaching flow before letting it go downstream. Flood waters possess a high kinetic head and may cause large scale damage. It is therefore, necessary to safely dissipate the energy of such a flow. Moreover, the information about the flow fields in such a case enables the engineers to effectively design the structures exposed to similar flows. The velocity profiles in vertical falls have been studied by many researches in the recent past [1]. Yet, most of the studies were experimental and theoretical. Theoretical analysis most accurately replicates the physical processes. But they are limited to a very specific range of applications that are rare in real world situations. Yet, these studies have helped engineers develop some of the state of the art technologies. On the other hand, experimental studies are the exact reflection of real world situations and hence form the

basis of validation of any theoretical model. Large amount of resources go into an experimental study and thus proves to be highly expensive and time consuming. With the development of computation power, numerical studies provide a more efficient way of modeling real world situations.

Most of the research in open channel hydraulics is focused on external flow velocity profiles. Extensive experimental studies in this area have been conducted by many researchers. Moore [5] studied the hydraulic characteristics of a free overfall and the dependence of energy losses at the fall on relative height of the drop during 1930's. This is when extensive studies in this field initiated. Rajaratnam and Chamani [6,7] measured the velocity profiles of falling and sliding jets of a fall over a vertical drop and also measured the energy loss for a flow over a stepped spillway. They came up with a theoretical formulation for average energy loss in a spillway as a function of flow parameters and geometry of the step. They later performed a series of experiments and proposed an equation for the drop in total energy based on experimental observation which is in the range of 43 – 68 %. Similar experimental investigation was performed by Chanson *et al*. [8] that focused on flow resistance in a vertical fall over a spillway. According to their study, flow resistance in a skimming flow is attributed to various factors, one of which is the interaction between recirculating cavities and the incoming jet. This is where the information about the velocity profiles in the recirculating zones plays an important role. Moreover, it is suggested in [9] that the flow over a stepped cascade can be studied as a series of vertically dropping pools. Recently, Lin *et al.* performed a series of experiments [2,3,4] at the Hydraulics Laboratory at National Chung Hsing University, Taiwan. These studies were focused on velocity profiles and flow field inside a vertically dropping pool. Laser Doppler Velocimetry was used to obtain the mean velocity profiles. They also proposed a characteristic velocity and length scale for deflected jet in

a vertically dropping pool based on their mean velocity field measurements as described in [4]. Formation and characteristics of the shear layer that develops in the jet were analyzed in [3]. Shear layers are formed due to the momentum exchange between the jet and the circulating fluid in the pool. Extensive mixing between the sliding jet and the pool contributes to the main energy loss in the dropping flow according to [5].

The various flow patterns in vertically dropping pools under subcritical approaching flow conditions were addressed in [2]. Depending on the approaching flow discharge, velocity and geometry of the drop structure, five types of flow patterns were identified which include a napped flow, a transitional flow between napped and periodically oscillatory flow, a periodically oscillatory flow, a transitional flow between periodically oscillatory and skimming flow and a skimming flow. Napped flow occurs when the falling jet impinges into the pool and thus causes high air entrainment. If the discharge becomes sufficiently large the dropping flow may slide over the circulating fluid in the pool which results in a skimming flow. Skimming flow possesses high momentum downstream and fewer amounts of air bubbles. The periodically oscillatory flow occurs for intermediate flow discharges. In general an oscillatory flow is perhaps the most undesirable type of flow in open channels and vertical drops. Yet, there are some exceptional situations where the oscillatory behavior proves to be useful. Air entrainment enhances the dissolved oxygen in the water and may be used for aquatic life and agricultural purposes. A highly effective way of using this effect in developing a Green Aerator is proposed in [2].

1.3 Experimental Techniques

As indicated previously, most of the research conducted in this area has remained experimental. Various methods, techniques and equipment have been used to accurately measure the flow field. Two of the most widely used techniques are Laser Doppler Velocimeter (LDV) and Particle Image Velocimeter (PIV). LDV measures the velocity of fluid particles moving perpendicular to a pair of coherent laser beams. Doppler Effect is observed in the waves scattered by these particles. The frequency of scattered radiation is proportional to the speed of particles.

Experimental studies done on the flow field in a vertically dropping pool [2,3,4] use a high speed camera with the PIV setup to measure the mean velocities within a specified region of focus called Field of View (FOV). PIV system for the experiments discussed in this study consists of a 5 W argon-ion laser as the light source. A mirror and a glass cylinder converted this light source into a thin sheet of light which is then allowed to pass through the transparent glass bottom of the experimental setup. Aluminum particles as small as 10μm in diameter were used as seeding material in the PIV. The settling velocity of the small aluminum particles is about 10μm/s, which is far less than the velocity of the concerned fluid. A schematic diagram of a PIV setup for this particular experiment is shown in Figure1-2. The findings of Lin *et al*. [3,4] show excellent agreement to the data obtained by LDV.

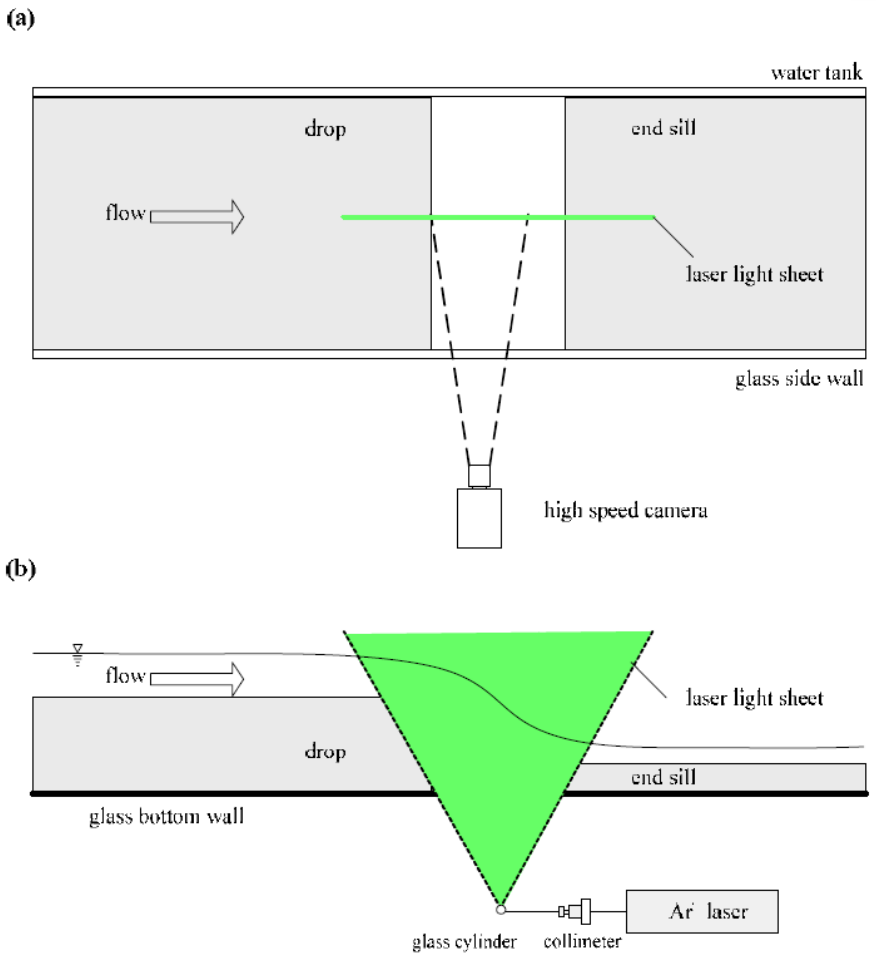

Figure 1-2 Schematic Setup for PIV [4]

A high speed camera was used to capture the instantaneous particle images. Using these images, the velocity field is then determined by cross-correlation analysis. Images were taken from three FOV's as shown in Figure 1-3. The high speed camera captures images at about 1000 frames per second which produces high spatial as well as temporal resolution. The free surface of the incoming and dropping flow was measured by flow visualization and also verified by a vernier point gauge. A sample image of the flow obtained from PIV is shown in Figure 1-4.

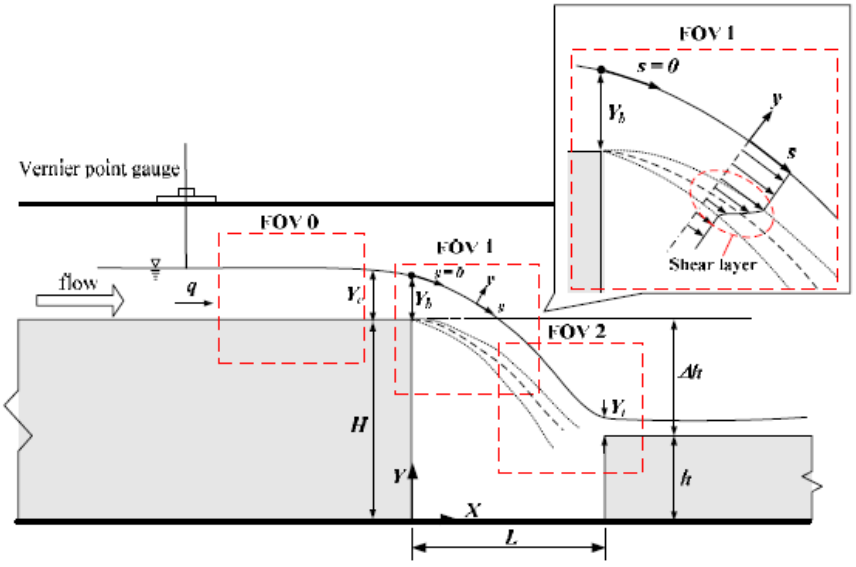

Figure 1-3 Fields of View for PIV system [4]

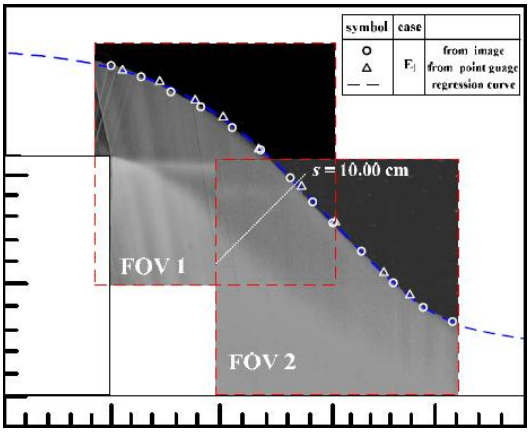

Figure 1-4 PIV Image [4]

1.4 Theoretical Information

1.4.1 Description of flow regimes

The present study focuses on an incompressible flow over a vertically dropping pool. The flow is considered incompressible because of its application to open channel hydraulics. The incoming flow is steady and subcritical but at the brink of fall it is supercritical. This jet impinges on the base of the pool and splits into two streams, one of the streams contributes to the development of a recirculation zone upstream just below the incoming jet and the other one goes downstream. The completely developed steady flow has just one recirculation zone which is typical of a skimming flow. The upper portion of the recirculation zone interacts with the incoming jet and thus increases the flow velocity in that region. However, the extent of this region is limited. The portion of the incoming flow which is under the influence of the recirculation zone is called a shear layer. Figure 1-5 shows the presence of a shear layer in a typical skimming flow.

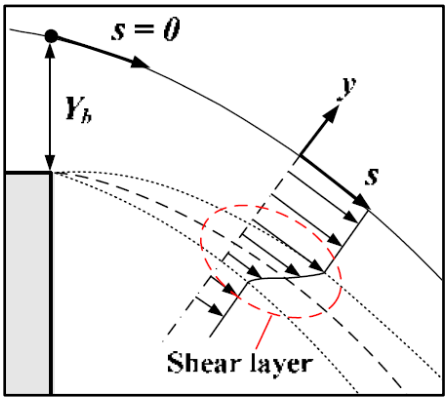

Figure 1-5 Shear layer in a falling jet

The previous discussion assumes that there is no obstacle in the downstream path of the flow. The scenario is quite different if there is an end sill close to the point of impingement of the falling jet. Its presence has a significant influence on the flow itself, in

addition to the flow field and shear layer. Depending on the location of the end sill, there can be two recirculation zones on either side of the impinging jet. The flow over a vertical fall with the presence of an end sill can be classified into three basic regimes based on the nature of the two recirculation zones. If the end sill is at a sufficient distance from the point of impingement, yet close enough to form another recirculation zone, the flow is called a Napped Flow. It implies that the two recirculation zones have independent influence on the incoming jet and that the two shear layers do not interact with each other. This kind of flow is steady when it is fully developed. If the incoming flow velocity is too high, unlike the case of napped flow where the end sill is far downstream from the point of impingement, it is seen that there exists only one recirculation zone beneath the incoming jet. The other recirculation zone is virtually absent. It indicates that the end sill is too close for the flow to be influenced by it. The flow profiles are similar to a case of skimming flow. Hence, it can be interpreted that the flow in this case essentially bypasses the end sill and behaves as if it were absent. Thus, low flow rates result in a napped flow and higher flow rates generate a skimming flow.

But there exists another flow regime for intermediate flow rates. If the velocity of the fluid (and thus the flow rate) is such that it creates two recirculation zones but not enough to neglect the effect of end sill, a periodically oscillatory flow results. In this case, strengths, and hence the size, of the two recirculation zones keeps changing periodically. As illustrated in Figure 1-6, after the formation of the two recirculation zones, the presence of end sill and a high enough velocity of incoming jet tend to strengthen the downstream vortex. The point of impingement tends to move closer to the wall. After a certain extent the vortex beneath the incoming flow gets strengthened due to a closer jet with a high velocity. This effect tends to move the jet away from the wall. Hence an

oscillatory behavior is created between the two recirculation zones and its effect is seen on the point of impingement of the jet. Shear layers are also similarly affected.

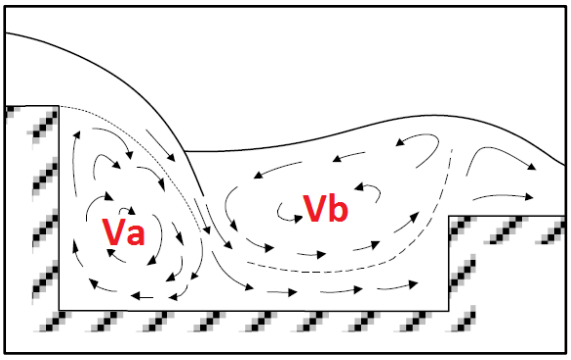

Figure 1-6 Recirculation zones due to presence of end sill

1.4.2 Energy curve and Froude Number

Discussions on open channel flows always relate to the state of flow that is being studied. Gravitational forces play an important role in any open channel flow and hence the state of flow is vital. The state of flow is defined by the Froude number which relates the inertia forces to the gravitational forces acting on a flow. It can also be seen as a ratio of characteristic velocity to the wave velocity of flow. For a flow within a uniform rectangular cross section, Froude number is given by:

$$Fr = \frac{V}{\sqrt{g\,D}} \tag{1}$$

where V is the flow velocity, D is the depth of flow and Uc = $\sqrt{g\,D}$ gives gravitational wave velocity which is also called critical velocity for open channel flows. The state of flow can be categorized as:

$$\text{Fr} \begin{cases} < 1 & \text{Subcritical (V <Uc)} \\ = 1 & \text{Critical (V = Uc)} \\ > 1 & \text{Supercritical (V >Uc)} \end{cases}$$

The specific energy i.e. energy per unit mass for a flow with velocity V and depth y can be expressed by Eq. (2):

$$E = y + \frac{V^2}{2g} = y + \frac{Q^2}{2g(y * 1)^2} \tag{2}$$

where Q is the flow rate and 'y*1'the is cross sectional area of rectangular channel with unit depth. Figure 1-7 shows a plot of specific energy vs depth of flow for constant flow rate. Point C corresponds to critical flow.

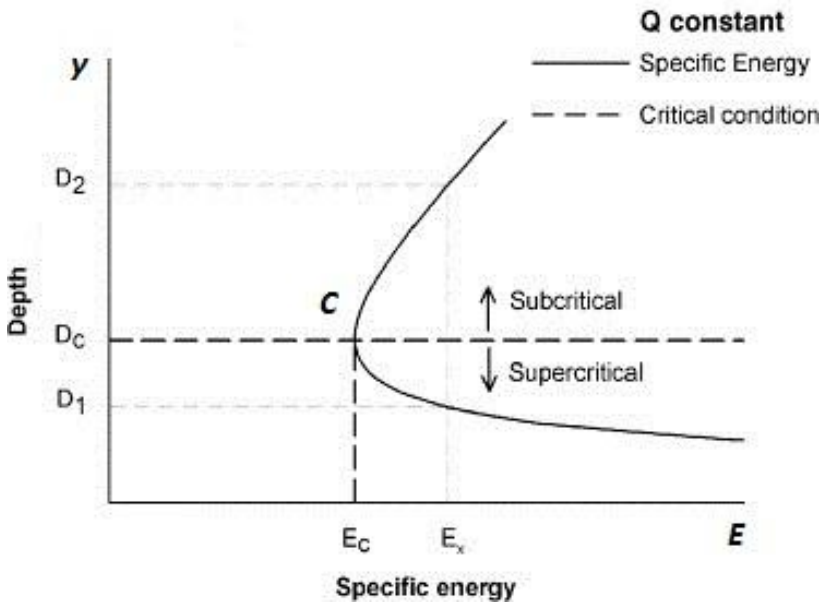

Figure 1-7 Specific Energy curve

At point C, the specific energy of the flow is minimum, which means that $\frac{dE}{dy}$ = 0. Differentiating Eq. (2) with respect to y and equating to zero, the following relation between kinetic head and pressure head is obtained.

$$\frac{V^2}{2g} = \frac{D}{2} \tag{3}$$

Eq. (3) shows that at the state of minimum energy, the kinetic head is half the hydraulic depth. Rearranging the terms, it can be shown that Fr =1 at C. In other words, critical flow corresponds to that state of flow beyond which the kinetic head becomes the dominant portion of the total specific energy [10].

1.5 Objective of Present Study

Numerical techniques provide an efficient way to model the realistic physical phenomena based on the governing equations and a mathematical model representing those. As mentioned earlier, theoretical analysis is often limited to very restrictive and idealistic assumptions of the processes while an experimental study most closely reflects the actual phenomena but proves to be expensive, time consuming and also takes up a lot of resources. Hence, with the development of computational power in the latter half of the the 20th century, numerical formulation, models and simulations became more popular. Numerical models and techniques are derived from theoretical principles but with some mathematical approximations.

The present study deals with numerical analysis of flow fields in three different types of flow regimes that take place in a vertically dropping pool. Generally a skimming flow is generated in such a situation with one recirculation zone and a developing shear layer. The presence of an obstacle results into another recirculation zone which in turn affects the velocity profiles in the shear layer. Depending on the nature of the recirculation zones, the flow is categorized as napped, oscillatory and skimming flow. The type of flow taking place in a particular situation depends on the velocity and depth of flow which are governed by the Froude number. The objective of this study is to

numerically model the three flow regimes. Velocity profiles in the recirculation zones and the shear layer are examined and compared with experimental findings reported in [2,3,4].

A detailed description about the numerical techniques used for solving governing equations and tracking of the free surface is presented in the next chapter. The subsequent chapters deal with the problem setup and description, discussion and analysis of the numerical results and comparison with experimental findings. In the end, a conclusion about the study is presented with some comments about prospective scope of research in this area. Code implementation, input file and numerical data are included in the appendix along with other relevant information.

Chapter 2

Numerical Formulation

2.1 Introduction

The basic idea behind any numerical scheme is to divide the whole physical domain into small elements or volumes and then solve the governing equations pertaining to those discretitized cells. Finite Element and Finite Volume are the two widely used numerical schemes. Finite volume approach is generally preferred for applications involving fluid flows. Open channel flows are a typical application of fluid dynamics to incompressible fluids. Numerical analysis in open channel flows can be used to perform various analysis like to get a pressure and flow field, hydrodynamic forces acting on dams and river beds which affect the sedimentation and aquatic life in some cases. These data prove to be useful in preserving natural water resources and also crucial applications like flood prevention. Moreover, hydroelectricity is a developing field of fluid science, open channel hydraulics and fluid power engineering which involves extensive use of numerical techniques to model the flow and optimize the hydroelectric power generation. Thus numerical techniques do have a wide range of application in open channel hydraulics, but there also exists a major challenge in modeling such flows. Open channel flows are classified as moving boundary problems which means that the tracing of the free surface becomes difficult. In the subsequent sections, a technique called Coupled Level Set and Volume of Fluid (CLSVOF) method is described which is used for the free surface tracking.

Numerical analysis and simulations are widely used today because of their advantages over experimental and analytical solutions. Yet, experimental investigations are still needed to validate the numerical results. But numerical analysis proves to be highly efficient for carrying out parametric studies, elementary design calculations, failure

analysis etc. The algorithm used for this study involves two broad steps. First is to solve the governing equations and second is to track the free surface. A Finite Volume scheme on a fixed uniform grid is used for solving the governing equations and a CLSVOF method to track the free surface. A brief overview of the scheme is given here. Details of the numerical formulation can be found in [11,12,13,14].

2.2 Governing Equations

The fluid flow in open channel hydraulics is considered to be incompressible and is governed by the continuity equation and the Navier-Stokes equation given by:

$$\nabla \bullet \vec{V} = 0 \tag{4}$$

$$\frac{\partial \vec{V}}{\partial t} + \nabla \bullet (\vec{V}\vec{V}) = -\frac{1}{\rho}\nabla p + \frac{1}{\rho}\nabla \bullet \tau + \vec{g} + \frac{1}{\rho}\vec{F}_b \tag{5}$$

where $\vec{V}$ is the velocity, ρ the density, p the pressure, τ the viscous stress tensor and $\vec{g}$ the gravitational acceleration. $\vec{F}_b$ is the body force term which is used to model surface tension using the pressure boundary method (PBM) as explained in [12,13,14]. For Newtonian fluids, the stress tensor, τ , can be expressed using Eq. (6).

$$\tau = 2\mu S \tag{6}$$

where μ is the dynamic viscosity and S is the strain rate tensor given by:

$$S = \frac{1}{2}\left[\left(\nabla \vec{V}\right) + \left(\nabla \vec{V}\right)^T\right] \tag{7}$$

As seen above, the governing equation is a partial differential equation dependent on both, time and spatial coordinates. Hence, it needs to be discretized in time first as shown in Eq. (8).

$$\frac{\vec{V}^{n+1}-\vec{V}^{n}}{\delta t}=-\nabla\bullet(\vec{V}\vec{V})^{n}-\frac{1}{\rho^{n}}\nabla p^{n+1}+\frac{1}{\rho^{n}}\nabla\bullet\tau^{n}+\vec{g}^{n}+\frac{1}{\rho^{n}}\vec{F}_{b}^{\,n} \tag{8}$$

where the superscripts n and n+1 represent the value of the variable at consecutive time steps. The only implicit term in the above equation is the pressure gradient. Gravity, advection, surface tension and viscosity are approximated with old time t^{n} values. A two-step projection method is used to separate the above equation into two as:

$$\frac{\tilde{\vec{V}}-\vec{V}^{n}}{\delta t}=-\nabla\cdot\left(\vec{V}\vec{V}\right)^{n}+\frac{1}{\rho^{n}}\nabla\cdot\tau^{n}+\vec{g}^{n}+\frac{1}{\rho^{n}}\vec{F}_{b}^{\,n} \tag{9}$$

$$\frac{\vec{V}^{n+1}-\tilde{\vec{V}}}{\delta t}=-\frac{1}{\rho^{n}}\nabla p^{n+1} \tag{10}$$

An intermediate velocity $\tilde{\vec{V}}$ between *n* and *n+1* time step is considered. The initial change in velocity is attributed to gravity, advection, surface tension and viscosity which are all explicitly known. The latter change comes from the pressure gradient only which is implicit. Thus there are two steps involved in solving this governing equation. In the first step of the projection method, an intermediate velocity field $\tilde{\vec{V}}$ is computed from Eq. (9). The second step involves taking the divergence of Eq. (10) while imposing the incompressibility condition on the velocity field. As a result, following pressure Poisson equation is obtained.

$$\nabla\cdot\left[\frac{1}{\rho^{n}}\nabla p^{n+1}\right]=\frac{\nabla\cdot\tilde{\vec{V}}}{\delta t} \tag{11}$$

It can be solved by incomplete Cholesky Conjugate gradient method [15] to obtain the pressure and hence the velocity field for subsequent time step.

2.3 Review of Interface/Free Surface Tracking Methods

The tracking of free surface in open channel flows poses a problem because they fall under the category of moving boundary problems. It becomes difficult to accurately locate and model the free surface or an interface if it undergoes drastic topological changes during the course of the flow. There are a few techniques developed to accomplish this. These can be broadly classified as Lagrangian methods and Eulerian methods [16]. Lagrangian based methods track the interface explicitly by treating the interface points as particles and the exact location of the interface is obtained directly by solving the equations of motion of these particles. Some of the examples of this method are moving grid, front tracking, boundary integral and particle-based methods. In the Eulerian method, the interface is represented by an appropriate field function, which is advected in time while solving the governing equations. The interface is then reconstructed depending on the properties and behavior of this field function. This category includes continuum advection, volume tracking, level set, and phase field methods.

The algorithm used for this study uses the Eulerian approach. It makes use of both Volume of Fluid and Level Set methods for accurately tracking the free surface. Hence it is called the Coupled Level Set and Volume of Fluid method. A Piecewise Linear Interface Construction (PLIC) scheme is used to reconstruct the free surface. A complete description about this technique is presented after a brief review about each of the individual methods.

2.3.1 Volume of Fluid (VOF) method:

The Volume of Fluid method is developed from the Marker and Cell (MAC) technique. MAC was developed by Francis Harrow and the Los Alamos National Laboratory [17]. It uses small grids like any other finite volume scheme along with

particles called markers that give information about the location of the free surface. A similar concept is used in the VOF method [18] that was developed in 1976. In this method, the markers are replaced by a scalar function F (x,y,z,t) which denotes the fraction of cell which is occupied by fluid. 'F' is essentially the ratio of volume of fluid to the volume of cell. Following interpretation about a particular cell can be made from the corresponding value of VOF function 'F'.

$$F(x,y,z,t) \begin{cases} = 0 & \text{Cell is in the void region} \\ 0 < F < 1 & \text{Cell is at the interface} \\ = 1 & \text{Cell is in fluid} \end{cases}$$

An example for the VOF functions representing a circular fluid element is shown in Figure 2-1. The number in each cell denotes the volume fraction occupied by the liquid. The VOF functions are advanced by the following propagating equation.

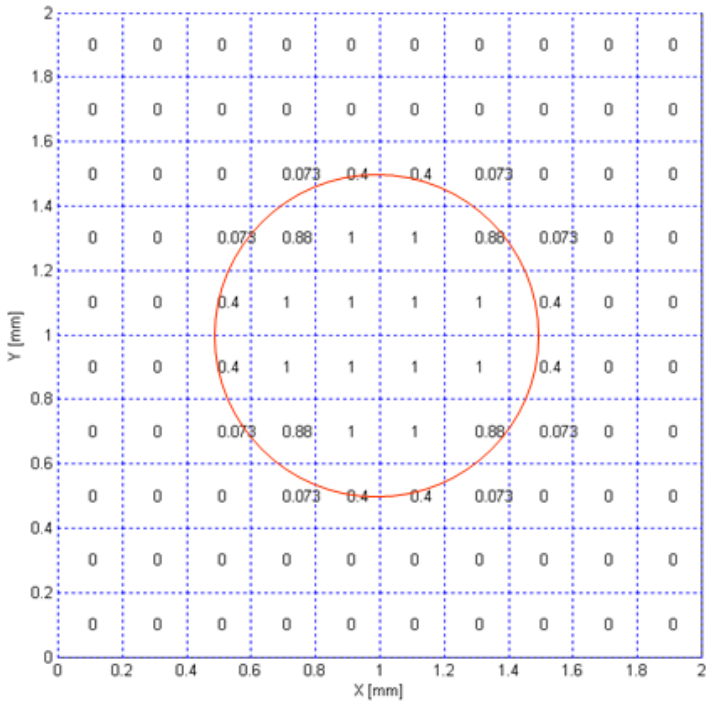

Figure 2-1 Volume of Fluid function for a circular fluid element

$$\frac{D}{Dt}(F) = 0 \tag{12}$$

Eq. (12) can be used in the conservative form to ensure mass conservation for all cells including the interface cells as follows:

$$\frac{\partial F}{\partial t} + \nabla \bullet (\vec{V}F) = F(\nabla \bullet \vec{V}) \tag{13}$$

It is discretized in time using an approach similar to the one used for solving the governing equations.

$$\frac{\tilde{F} - F^n}{\delta t} + \frac{\partial}{\partial x}\left(uF^n\right) = \tilde{F}\frac{\partial u}{\partial x} \tag{14}$$

$$\frac{F^{n+1} - \tilde{F}}{\delta t} + \frac{\partial}{\partial y}\left(v\tilde{F}\right) = F^{n+1}\frac{\partial v}{\partial y} \tag{15}$$

where $\tilde{F}$ is the intermediate VOF function. On the staggered grid, the VOF function, *F*, is located at the cell center and velocities, *u* and *v*, are stored at the cell edges, as shown in Figure 2-2. Discretizing the above equations spatially and integrating over a computational cell (i, j) yields:

$$\tilde{F}_{i,j} = \frac{F^n_{i,j}\delta x_i \delta y_j - \delta t \delta y_j \left(flux_{i+\frac{1}{2},j} - flux_{i-\frac{1}{2},j} \right)}{\delta x_i \delta y_j - \delta t \delta y_j \left(u_{i+\frac{1}{2},j} - u_{i-\frac{1}{2},j} \right)} \tag{16}$$

$$F^{n+1}_{i,j} = \frac{\tilde{F}_{i,j}\delta x_i \delta y_j - \delta t \delta x_i \left(flux_{i,j+\frac{1}{2}} - flux_{i,j-\frac{1}{2}} \right)}{\delta x_i \delta y_j - \delta t \delta x_i \left(v_{i,j+\frac{1}{2}} - v_{i,j-\frac{1}{2}} \right)} \tag{17}$$

where $flux_{i\pm 1/2,j} = (uF^n)_{i\pm 1/2,j}$ and $flux_{i,j\pm 1/2} = (v\tilde{F})_{i,j\pm 1/2}$. They denote VOF fluxes across the edges of the computational cell. The calculation of the fluxes at cell edges

requires an interpolation scheme for VOF functions which is described later. One important point worth noting about the VOF scheme is that it only calculates the values of F and does not give any information about the orientation of the free surface or the interface. Generating an interface from the VOF data alone would result into discontinuities between neighboring cells. In other words, the circular profile shown in Figure 2-1 cannot be obtained from VOF data alone. VOF scheme is highly accurate in locating the free surface and conserving the mass in each cell but fails to identify the orientation of the free surface.

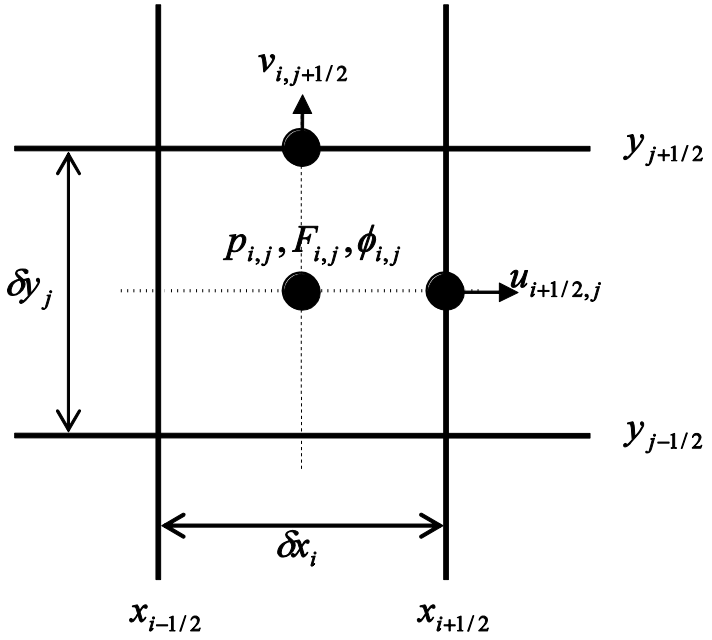

Figure 2-2 Staggered Grid

2.3.2 Level Set (LS) method:

This method was developed by James Sethian and Stanley Osher [19,20] during the late 1980's. The level set function φ is defined as a signed function whose magnitude is equal to the shortest distance of cell center from the interface or free surface. Following information can be drawn from the level set function.

$$\varphi\,(x,y,z,t) \begin{cases} > 0 & \text{Cell center is outside the fluid} \\ = 0 & \text{Cell center is at the interface} \\ < 0 & \text{Cell center is inside the fluid} \end{cases}$$

Following example (Figure 2-3) shows the use of Level Set function for a circular fluid element. The positive values indicate that the cell center is outside the fluid element while negative values indicate that it falls within the fluid.

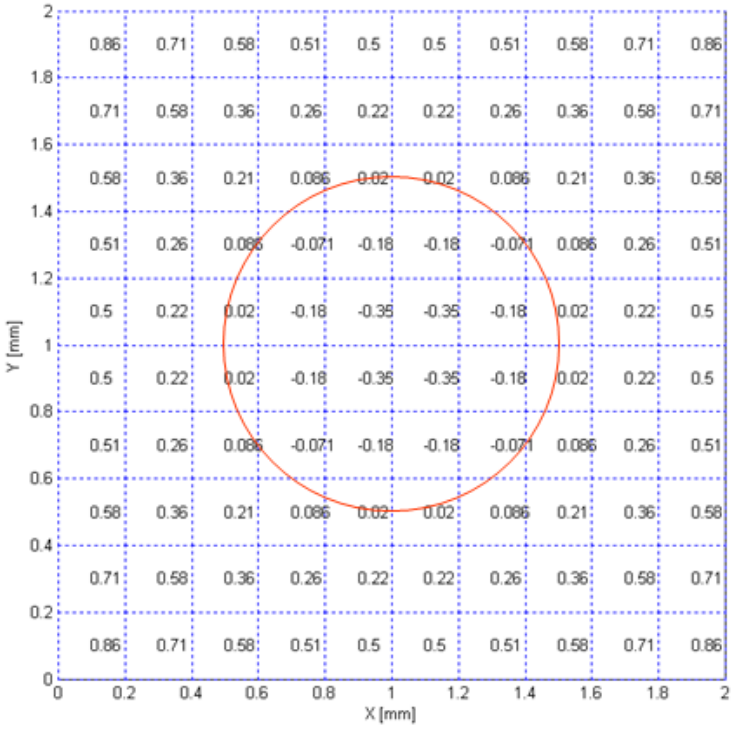

Figure 2-3 Level Set function for a circular fluid element

Another important property is that gradient of the level set function gives a unit vector normal to the interface. Thus,

$$\vec{n} = \frac{\nabla \phi}{|\nabla \phi|} = \nabla \phi \tag{18}$$

$$|\nabla \phi| = 1$$

This information is used to initiate the levels set function and then it is advected using the following form, which is same as discussed above.

$$\frac{\partial \phi}{\partial t} + (\vec{V} \bullet \nabla)\phi = 0 \tag{19}$$

Solving the above equation for subsequent time steps is easy and can be achieved by using appropriate advection schemes. But φ is a distance function which is not related to the fluid properties and hence Eq. (18) will not be satisfied after advection and the errors keep on piling after each subsequent step. Hence the level set function needs to be re-initialized as follows:

$$\frac{\partial \phi}{\partial t} = \frac{\phi_0}{\sqrt{\phi_0{}^2 + h^2}}(1 - |\nabla \phi|) \tag{20}$$

where 't' is the artificial time, φo is the value of LS function from previous time step and h is the grid spacing. But in doing so, the mass conservation is no longer satisfied for interface cells unlike the VOF scheme. Hence the LS function has to be re-distanced in every time step to satisfy the mass conservation. [21] describes a re-distancing algorithm.

2.4 Coupled Level Set and Volume of Fluid Method and Interface Reconstruction

It is seen from earlier discussions that there exist certain limitations about using the Volume of Fluid method or the Level Set method. The VOF data accurately locates the free surface and is consistent with mass conservation but fails to identify the orientation of the free surface. On the other hand, LS function gives the orientation of free surface from the gradient of φ but advection of this function disturbs the mass conservation law. These facts lead the discussion towards using the positives from both these methods and reconstruction the free surface based on the combined information. This is the idea behind the Coupled Level Set and Volume of Fluid (CLSVOF) method [11,22].

But there are still some concerns in the VOF and LS methods that need to be addressed. The calculation of VOF data for each cell requires information about fluxes at cell faces which in turn requires the value of F at the cell faces. The level set function needs to be re-distanced to make it compatible with the mass conservation. Hence there is a need of a scheme that approximates a free surface or an interface based on the values obtained from VOF and LS data.

A Piecewise Linear Interface Construction (PLIC) scheme [23] approximates the free surface to be a straight line across the cell faces such that the volume of fluid remains consistent with the VOF data and is oriented in a direction which is consistent with the gradient of LS function. The direction is identified from the LS function as:

$$\vec{n} = \frac{\nabla \phi}{|\nabla \phi|} = \nabla \phi, \qquad \alpha = \tan^{-1}\left(\frac{n_y}{n_x}\right) \ (0 < \alpha \leq 2\pi) \tag{21}$$

An example of an interface constructed in a cell using PLIC scheme is shown in Figure 2-4. Figure 2-5 shows a flow chart demonstrating the steps involved in CLSVOF method [11].

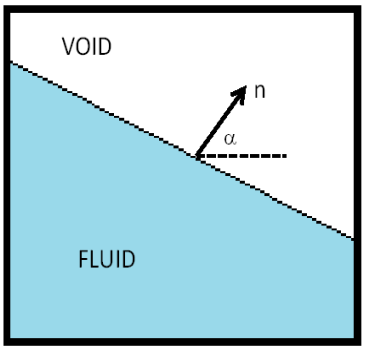

Figure 2-4 Example of Interface orientation obtained from PLIC scheme.

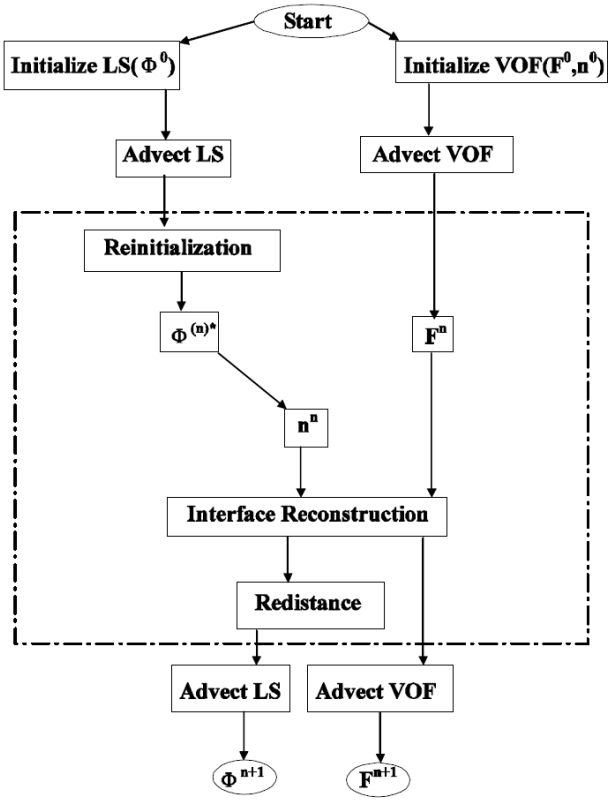

Figure 2-5 Flow chart of CLSVOF Algorithm [13]

Chapter 3

Problem Setup

3.1 Introduction

The numerical study of flow in a vertically dropping pool is a part of open channel hydraulics and is concerned only with incompressible flows. As mentioned earlier, the code uses a finite volume scheme on a fixed uniform grid in rectangular coordinate system. A grid sensitivity test has to be performed to decide the grid size that accurately models the flow. The free surface (interface) is obtained using the CLSVOF method with a PLIC scheme. The numerical and fluid parameters used in the study are included in the input file given in Appendix B.

3.2 Geometrical Setup

This study can be divided into two parts based on the geometry of flow domain. First part is about the flow over a vertically dropping pool without end sill and the second is with an end sill or obstacle. The first step involved in the problem setup is to create a geometric domain that represents the desired kind of flow without the loss of any information. Figures 3-1 and 3-2 show the geometrical setup of each part. The end sill in the second part is modeled as a rectangular obstacle to be consistent with the experimental investigations of Lin *et al.* [2,3,4]. Dimensions of these parts are taken in accordance with specific cases to be examined.

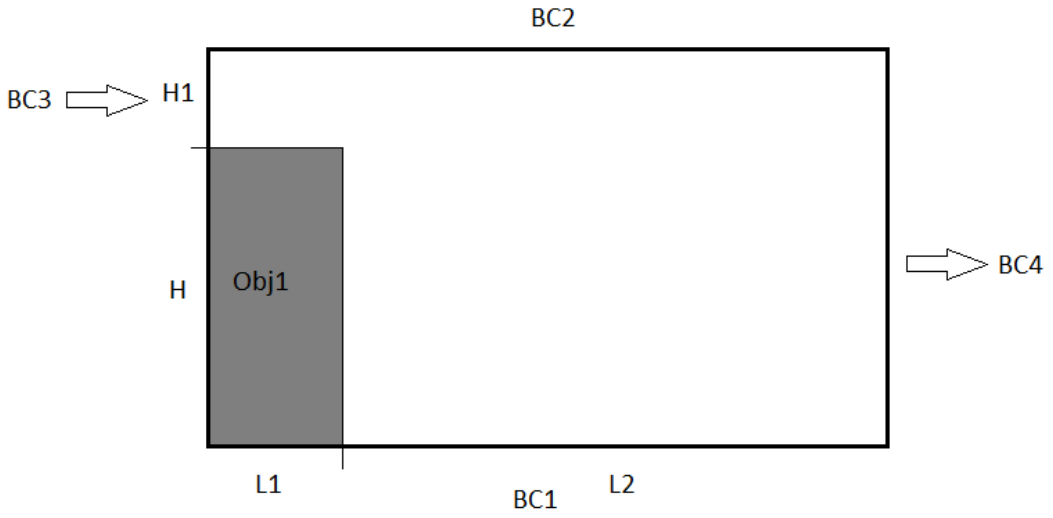

Figure 3-1 Geometry for Part 1 (No End Sill)

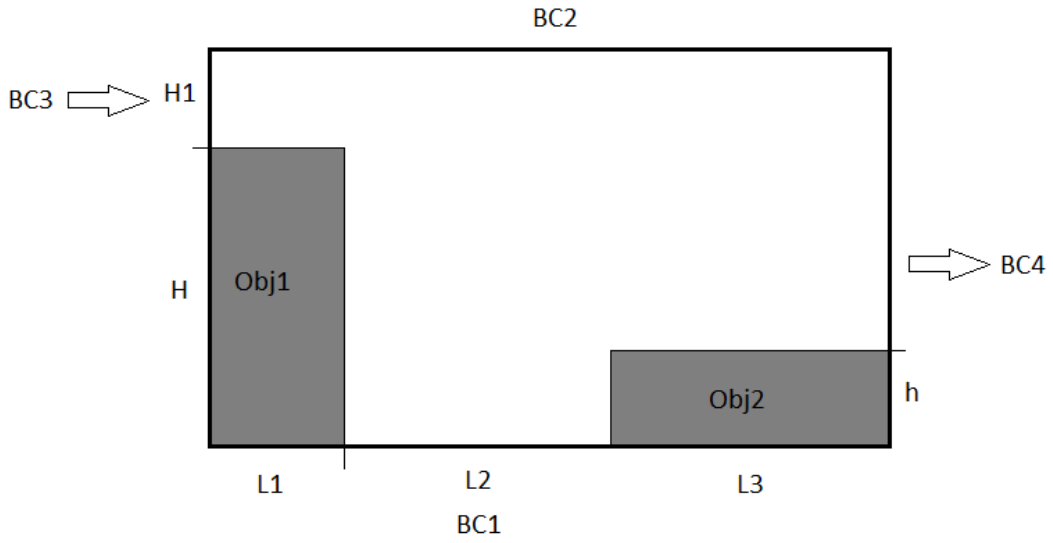

Figure 3-2 Geometry for Part 2 (With End Sill)

Obj1 is created to simulate a vertically falling flow. The arrows indicate the direction of flow at boundaries. 'H' is the height of fall. The length L1 plays an important role here. Recall the information from chapter 1 that a subcritical flow in an open channel converts into supercritical after a certain time. L1 is the length over which this transition takes place. The flow at the brink of fall has to be supercritical which implies that L1 has to be sufficiently long for this transition to take place. L2 is the length of pool. In Figure 3-1 there is no obstacle. But this length is very significant in part 2 because that will affect the development of second recirculation zone above the incoming jet. An initial set of tests were performed to determine appropriate values of L1, L2 and L3. L2 which is the length of the pool was set to 80 mm and L1 was set in the range of 30 – 50 mm which is sufficiently large. L3 was set to be 50 mm so that the boundary conditions would not affect the solutions near the pool.

3.3 Boundary Conditions

Boundary conditions play an important role in any numerical simulation. The boundary conditions taken for these studies are summarized in Table 3-2.

Table 3-1 Boundary Conditions

Boundary	Type
BC1	Rigid No-Slip
BC2	Continuative Outflow (Any)
BC3	Specified Inflow
BC4	Continuative Outflow
Object edges	Rigid Free-Slip

Specified inflow condition defines the value of velocity at that face. Thus it is a value specified condition. Rigid No-Slip condition or Wall boundary implies that the velocity at the face is zero and there is no flow across that face. Continuous outflow means that the gradient of velocity in a direction perpendicular to that face is zero. The boundary condition at the inlet is more important because it will define all the parametric cases taken into consideration for this particular study. Note that all objects have a free slip boundary condition at the faces.

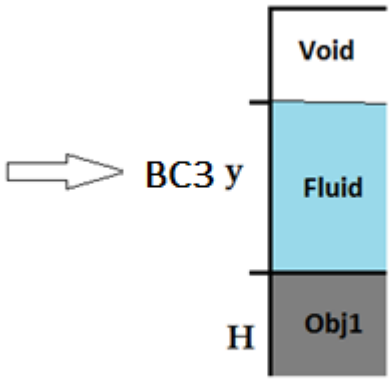

Figure 3-3 Boundary Condition at Inlet

The condition BC3 is only applied to the inlet region if height ‘y’. It has been found that the flow can be categorized into napped, skimming or oscillatory based on the ratio of fluid depth to the height of flow i.e. y/H. Thus, the cases for this study would have different y/H ratio. Another important parameter that controls the flow regime is h/H which is the ratio of height of end sill to the height of fall. But the present study is limited to the cases with h/H=0.43.

3.4 Parameters

As explained above, y/H is the parametric ratio that gives rise to different flow regimes. The study is divided into two parts as shown in Tables 3-2 and 3-3. The height of fall 'H' is set to 110 mm for part 1 and 70 mm for part 2. Flow rate is used to control the parameter y/H. y/H ranges from 0.4 to 0.6 for cases without end sill and from 0.2 to 0.3 for cases with end sill. Corresponding inlet and critical velocities, critical depth and Froude number are listed below.

Table 3-2 Parameters for Part 1 (No End Sill)

Case	H (mm)	q (cm^2/s)	y (mm)	U (m/s)	yc (mm)	Uc (m/s)	y/H	Fr
1A	110	304.00	47.50	0.640	45.52	0.67	0.43	0.958
1B	110	433.13	52.50	0.825	57.63	0.75	0.48	1.098
1C	110	500.25	57.50	0.870	63.44	0.79	0.52	1.103
1D	110	581.25	62.50	0.930	70.12	0.83	0.57	1.122

Table 3-3 Parameters for Part 2 (With End Sill)

Case	H (mm)	q (cm^2/s)	y (mm)	U (m/s)	yc (mm)	Uc (m/s)	y/H	Fr
2A	70	44.80	14.00	0.320	12.70	0.35	0.20	0.907
2B	70	49.50	15.00	0.330	13.57	0.36	0.21	0.905
2C	70	55.25	16.25	0.340	14.60	0.38	0.23	0.899
2D	70	60.35	17.00	0.355	15.49	0.39	0.24	0.911
2E	70	77.00	20.00	0.385	18.22	0.42	0.29	0.911

Chapter 4

Results and Discussion

4.1 Introduction

The series of experiments performed can be classified into two broad categories depending on the geometry or physical conditions. Firstly, the flow inside a vertically dropping pool without the presence of end sill is analyzed. In this case, the expected flow regime is only of skimming type. As mentioned in chapter 3, a wide range of experiments were carried out with different flow rates, depth of flow and velocities. These parameters are related by the Froude number. A broad picture of the flow field and free surface is presented. Later, the flow field and velocity distribution in the recirculation zone and shear layer are also studied. Next, the flow over a vertically dropping pool with the presence of an obstacle or end sill is studied. This is the case where three different flow regimes are observed with two recirculation zones. Velocity profiles in these recirculation zones and shear layer are presented. Moreover, a brief description about the oscillatory behavior of flow for a particular case is also presented. In the end, some comments about how the boundary conditions affect the numerical results are also made.

A grid refinement study was initially performed to determine the appropriate grid size for the domain. The grids have to uniform (square) as required by the CLSVOF scheme. A preliminary set of tests was performed with different grid sizes ranging from 5 mm to 0.5 mm. The simulation is advanced till the flow reaches the brink of fall which is a significant location where the overshoot velocity occurs. Figure 4-1 shows velocity plots with different grid sizes and a convergence is observed for grid sizes less than 1 mm. A set of parameters was figured out referring to literature and experimental tests previously performed. Appropriate changes were made to the subroutine for boundary conditions to accommodate the inlet conditions shown in Figure 3-3. After compiling this code and

executing it with corresponding input file (see appendix) a set of data files is generated that gives information about the flow field and free surface. This data is then post processed to obtain desired results.

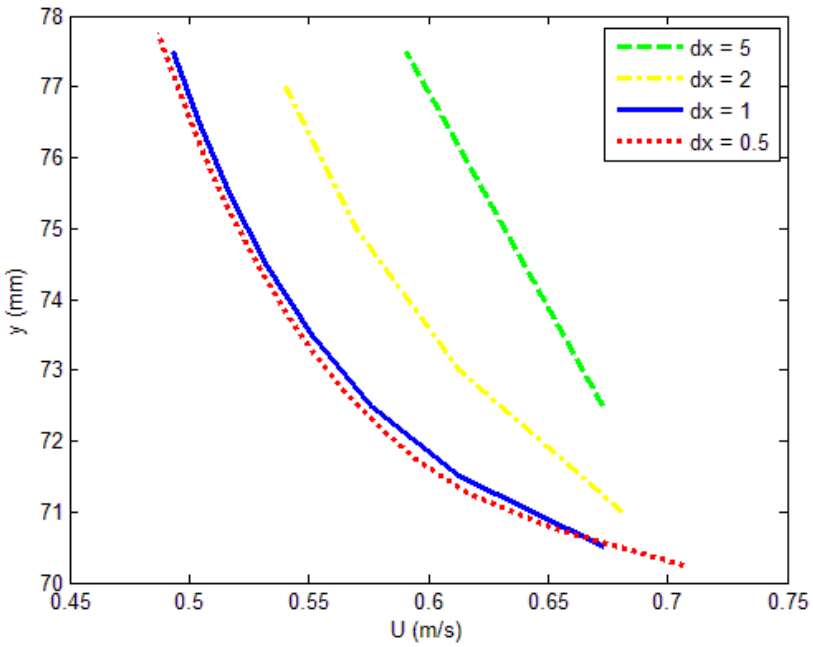

Figure 4-1 Grid Refinement test

4.2 Flow inside a vertically dropping pool without end sill

Incompressible fluid flow inside a vertically dropping pool generates a skimming flow with one recirculation zone. Figure 4-2 shows a typical skimming flow (case 1C). The vortex Va denotes the recirculation zone. The recirculation zone and stagnation point for this case are magnified and shown in Figures 4-3 (A) and (B) respectively. With the information about flow field, the velocity profiles in shear layer and recirculation zones can be examined. The location of center of recirculation zone and shear layer can also be determined from these analysis which are addressed in subsequent sections.

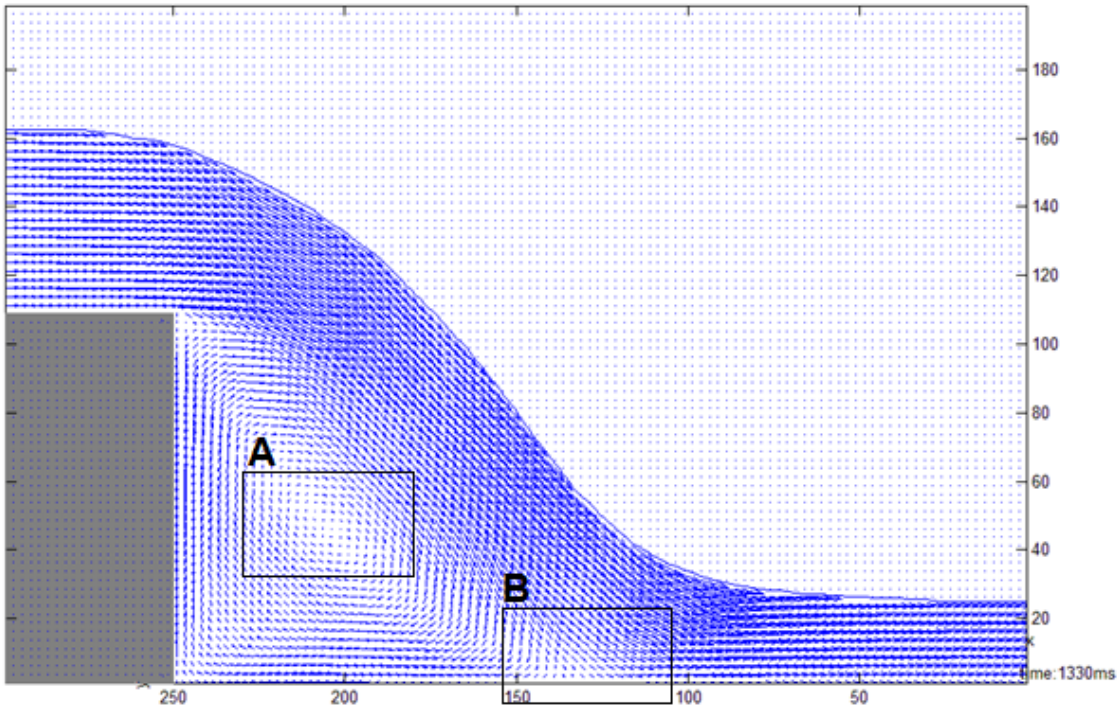

Figure 4-2 Typical skimming flow regime in vertically dropping pool without end sill

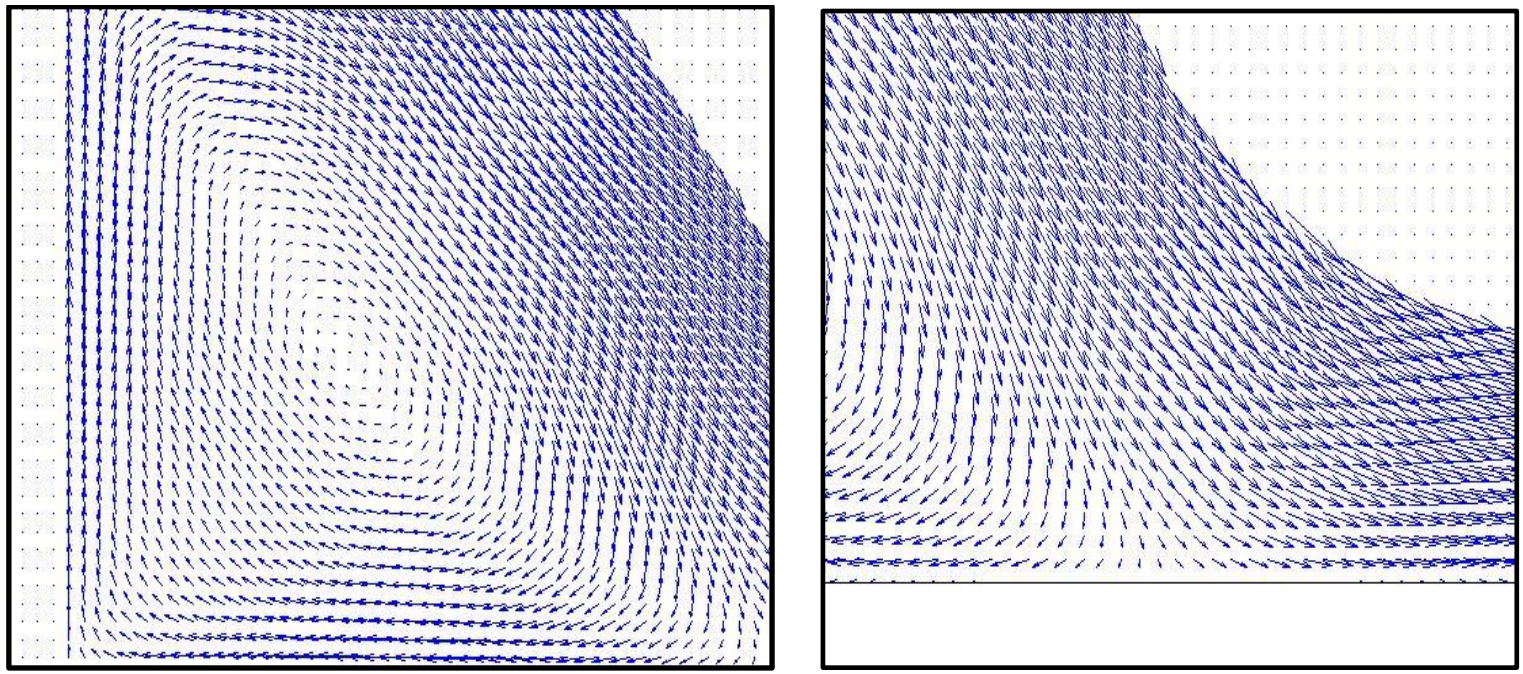

A B

Figure 4-3 Recirculation zone and Stagnation point

(A) Recirculation zone (B) Stagnation point

The velocity profiles in four different sections of the shear layer are studied and presented in Figure 4-4. These data correspond to case 1C (refer chapter 3). Section A corresponds to the location where the shear layer starts developing. The profile at this location is not at all affected by the recirculation zone and hence it is similar to that of a typical super-critical flow in an open channel. Location B corresponds to a section that passes through the center of the recirculation zone. C is a random location passing across the shear layer and D corresponds to the section that passes through the stagnation point.

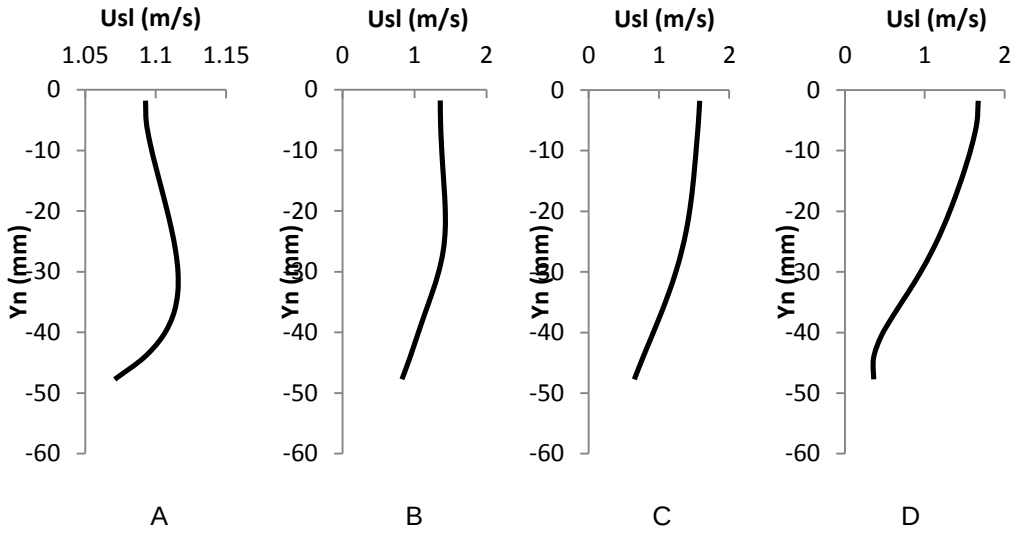

Figure 4-4 Velocity in shear layer at different locations (present study)

The profiles shown in Figure 4-4 correspond to the velocity profiles in the shear layer which are similar to what Lin et al. observed in [4]

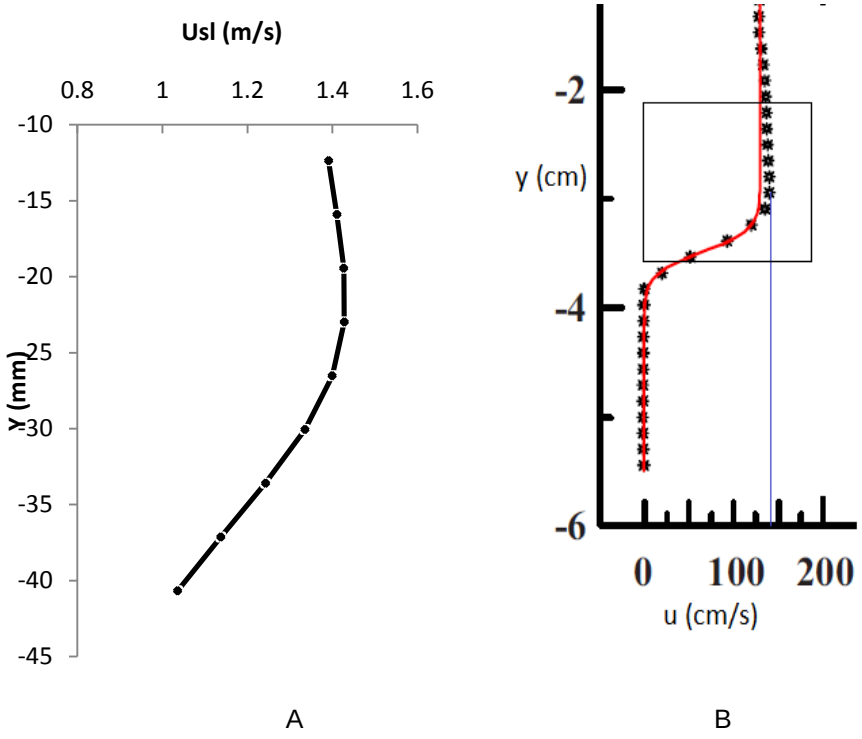

Figure 4-5 Interaction between sliding jet and recirculation zone

Figure 4-5 (A) shows an enlarged view of velocity profile in a shear layer. A small bump in the velocity profile is observed at y= -22.5 mm. This is due to the effect of the recirculation zone. The incoming jet interacts with the recirculation zone underneath it which has a clockwise circulation. Hence some portion of this zone which is just below the incoming jet contributes to the increase in the velocity in this region. This region is called the shear layer. Alternatively, it can be seen that the streamlines in this region are closer to each other (refer Figure 4-2) which implies that the velocity is higher. It is observed that the velocity above the shear layer is almost constant which can be explained by the fact that this portion of the jet is least affected by the circulation. The region below the shear layer has a uniformly decreasing velocity as it is a part of the recirculation zone. Figure 4-5 (B) is a plot at a similar location obtained from the

experimental studies of Lin *et al.* in [4]. At some location below the shear layer, it also changes direction. Subsequent sections will demonstrate a velocity profile in the recirculation zone. Percentage increase in velocity in shear layer obtained numerically is 4.9 % which agrees with experimental results found in [4] to be around 5.2 %.

The incoming flow may be sub-critical or super-critical depending on the Froude number. But, as it advances, its pressure head reduces and the velocity head increases. Hence, it becomes critical at some stage and further develops into super-critical range (Fr>1) downstream. This effect can be seen from the velocity plots at the incoming stream. The flow condition at the brink of the fall is super-critical (U>Uc). This means that the maximum velocity is greater than the critical velocity which is called overshoot. The overshoot always occurs in an open channel flow when a sub-critical flow converts into super-critical. Overshoot velocity is about 6-7 % higher than inlet velocity as observed from the numerical and experimental data. The numerically obtained velocity profile in a vertical section at the brink of fall is shown in Figure 4-6 (A) with its corresponding experimentally obtained plot [3] in Figure 4-6 (B). The nature of the profile is similar except for y < 11.5 cm. This is due to the boundary layer effect (see Chapter 5).

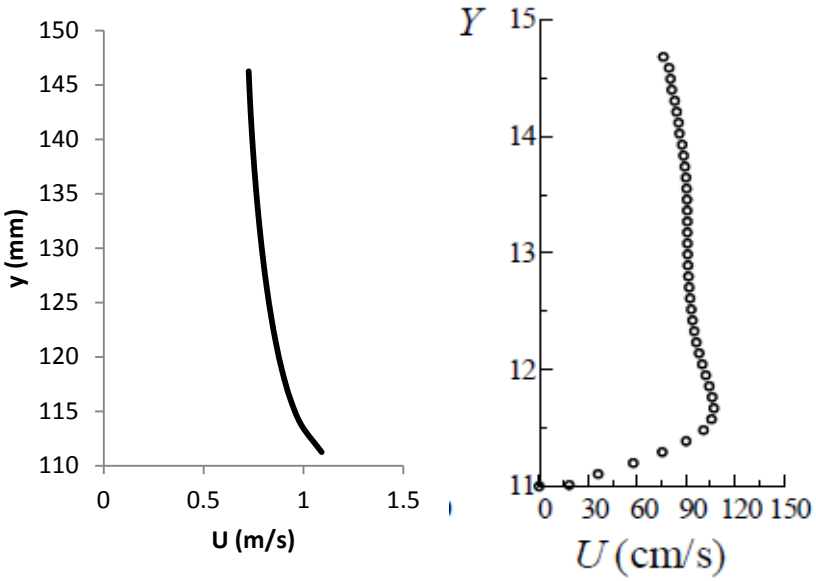

A B

Figure 4-6 Velocity in super-critical region at the brink of fall

(A) Numerical (B) Experimental [4]

As y increases, the velocity decreases to zero and then becomes positive above the center of the recirculation zone. In other words, the center of the recirculation zone is located at the point where the velocity changes direction. Moreover, it is seen from the plot that there is a slight increase in the horizontal velocity near the free surface. This is due to the presence of the shear layer (marked in red). Figure 4-8 shows the numerically obtained velocity profile for case 1C (yc/H = 0.52). It is seen that the velocity intersects the vertical axis at y=60 mm which marks the center of the recirculation zone and the increase in velocity near the top can be accounted for from the plots in Figure 4-4.

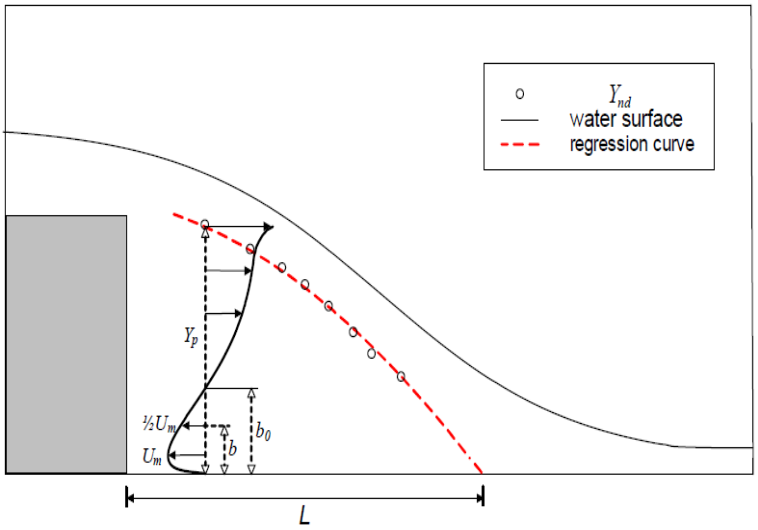

Figure 4-7 Location and velocity profile in recirculation zone (theoretical sketch)

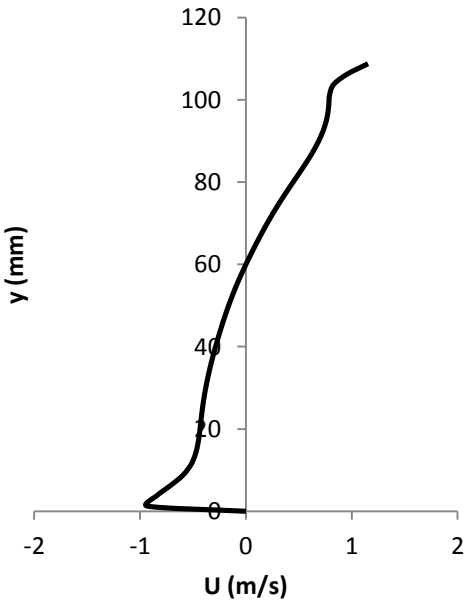

Figure 4-8 Velocity in recirculation zone (present study)

4.3 Flow in a vertically dropping pool with end sill

The presence of an end sill drastically changes the nature of flow in the pool. There can exist three different flow regimes in this case depending on the flow conditions as described in previous chapters. The series of tests done in this part of the study include flow parameters that would result in a napped flow, an oscillatory flow or a skimming flow. Velocity profiles in each case are studied. Figure 4-9 and Figure 4-10 show a napped and skimming flow. It should be noted that Figure 4-9 has two recirculation zones Va and Vb while Figure 4-10 has only one with Vb absent. It is because the flow rate and velocity are high enough to neglect the end sill (obstacle). Alternatively, it can be seen that the jet impinges on the end sill. This implies that the obstacle has no role to play in this case. Both napped and skimming flows are steady.

If the flow rate is within some specific range, an intermediate situation arises which results into an oscillatory flow as explained earlier. In this case, the strength and location of the recirculation zones keep changing over a period of time. It is observed that Vb reduces in size, completely vanishes and then reappears over the course of one complete cycle whereas Va moves towards and away from the incoming jet alternatively. A detailed study about these cases is presented here and the velocity profiles in the shear layer and recirculation zones were examined.

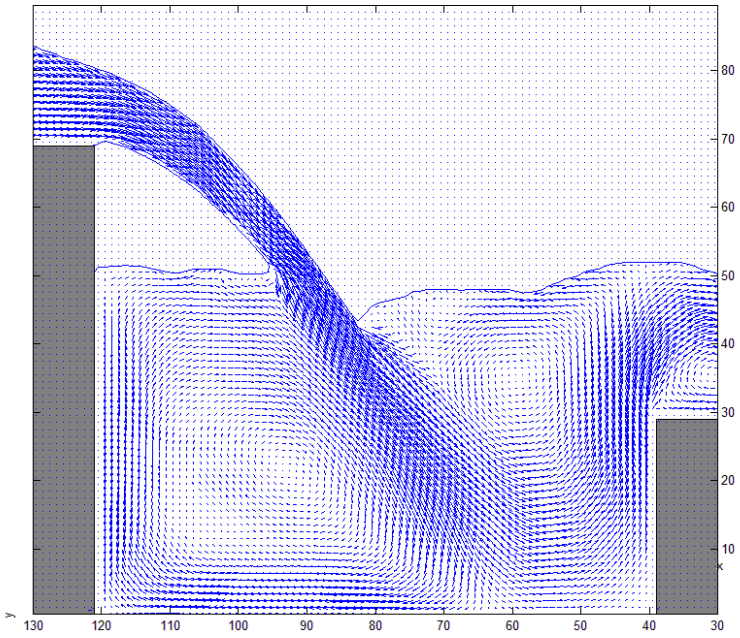

Figure 4-9 A Typical napped flow

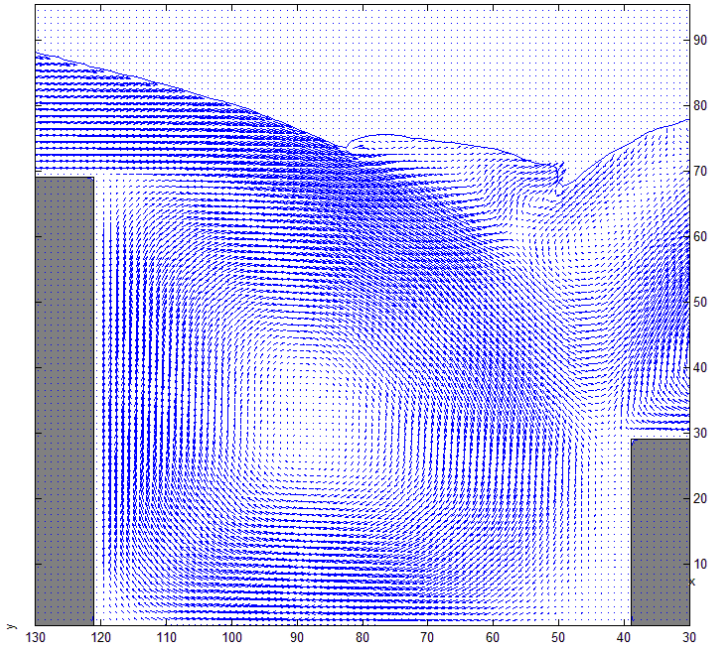

Figure 4-10 A Typical skimming flow

4.3.1 Napped Flow

A napped flow regime for case 2A (y/H=0.20) was analyzed and presented here. For this case, the velocity profiles in both the recirculation zones are studied. Along with that, the velocity profiles in shear layer are also presented. The shear layer in this case will be different from what was presented in section 4.2. This is because it is affected by two opposite circulations.

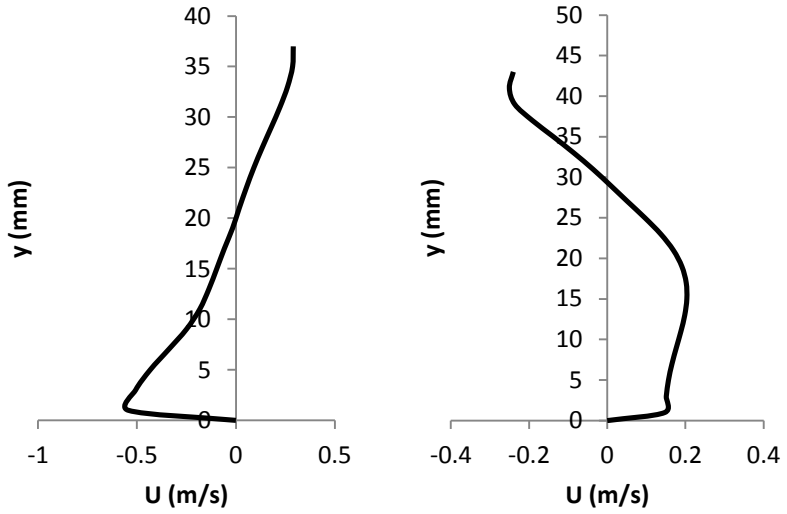

A B

Figure 4-11 Numerically obtained velocity in recirculation zones

Refering to Figure 4-7, it is observed that as the flow rate increases, the maximum velocity in negative x direction also increases. This indicates that the maximum velocity (Um) can be used to non-dimensionalize the velocity in the recirculation zone. Moreover, the center of the recirculation zone also moves up (towards the incoming jet) and hence ‘bo’ also increases with increase in flow rate. Thus, a similarity profile can be

obtained using the velocity ‘Um’ and a characteristic length ‘bo’ to non-dimensionalize the respective physical quantities. Figure 4-12 shows the similarity profile for cases 2A, 2B and 2C along with a similarity profile obtained experimentally from [3].

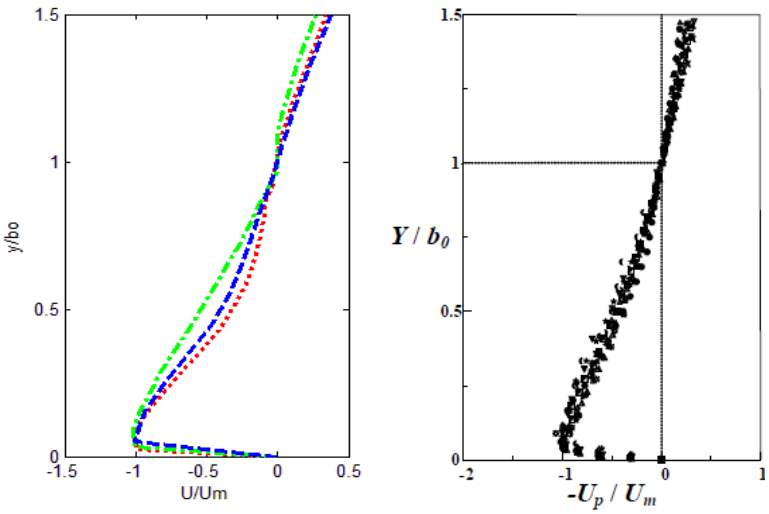

Figure 4-12 Similarity profile for velocity in recirculation zone

(A) Numerical (B) Experimental

The velocity profile within the shear layer for case 2A at section A (refer Figure 4-13) is presented in Figure 4-14. Figure 4-15 shows experimentally obtained plot in [3] It is observed that the nature of the graph is similar to one obtained for a skimming case. This is because the section A lies in the region where the shear layer is completely under the influence of only one recirculation zone. This profile does change when another section B is considered towards the right. Figure 4-16 shows the velocity in the shear layer at this section. The top portion of the layer is distorted as it is under the influence of oppositely circulating zones.

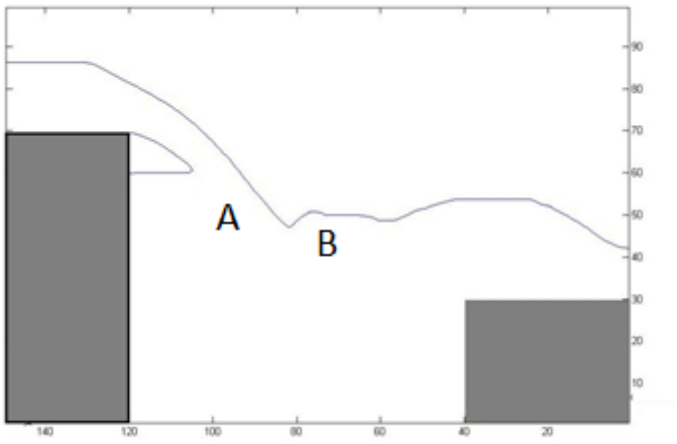

Figure 4-13 Sections A and B in the shear layer

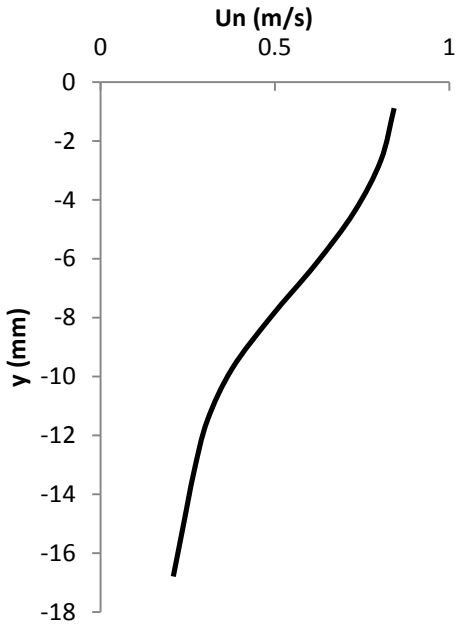

Figure 4-14 Numerically obatined velocity profile in shear layer (present study)

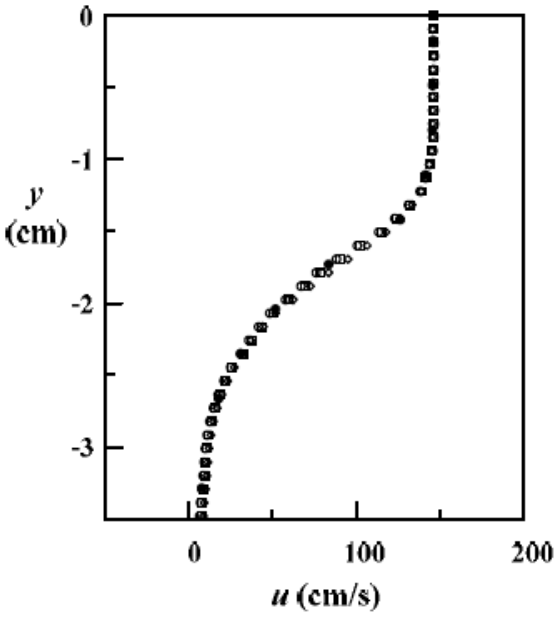

Figure 4-15 Nature of velocity distribution in shear layer observed experimentally [3]

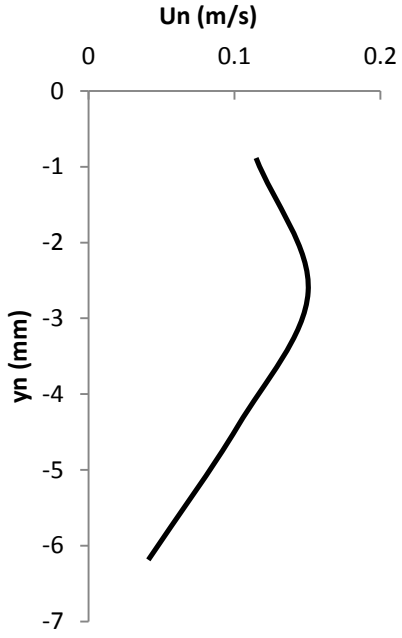

Figure 4-16 Numerically obtained velocity in shear layer at section B (present study)

4.3.2 Skimming Flow

For the case of skimming flow in a vertical pool with end sill, the velocity profiles are similar to what is presented in section 4.2. Following plots show these profiles for case 2E (y/H = 0.29). The velocity distribution in the shear layer obtained numerically for this case shown in Figure 4-17 (A) is similar to that obtained by Lin *et al.* in [3]. The velocity in recirculation zone shown in Figure 4-17 (B) is also same as what is obtained in section 4.2.

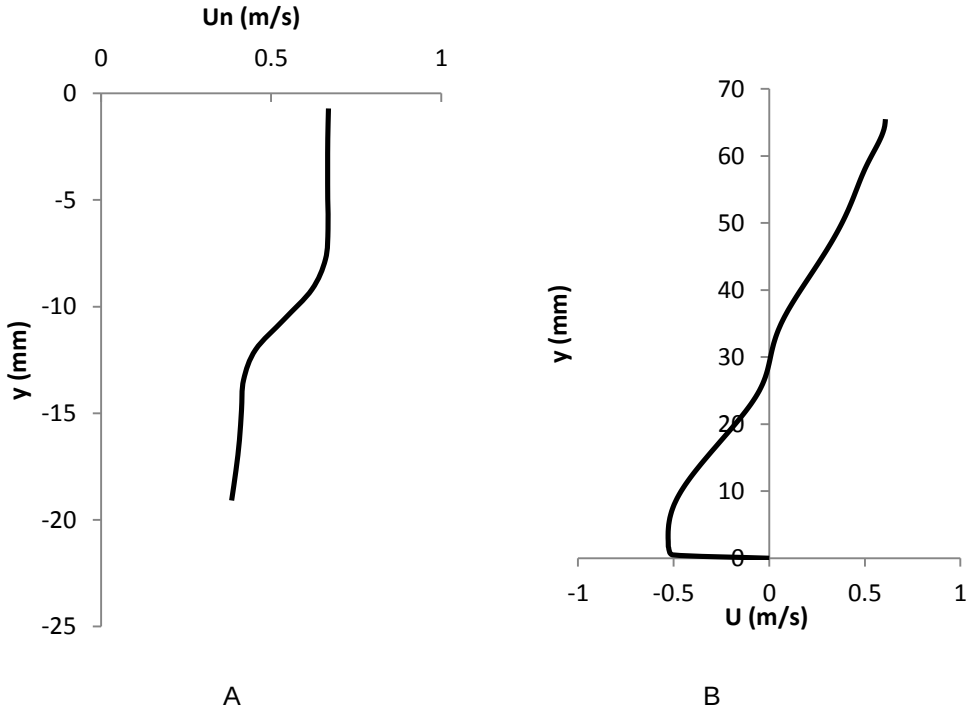

Figure 4-17 Velocity in shear layer and recirculation zone for skimming flow (present study)

(A) Shear Layer (B) Recirculation zone

4.3.3 Oscillatory Flow

The third case is a periodically oscillatory flow. As described previously, the two recirculation zones keep changing their size periodically. Figure 4-19 depicts the variations in one complete cycle for case 2D (y/H=0.24). The total time taken for one complete cycle is 1800 ms. (1.8 s). Hence,

$$f = \frac{1}{T} = 0.555\ Hz$$

where T is the period of one complete cycle. It is reported in [2] that this fundamental frequency is close to 0.55 Hz. Figure 4-18 shows the initial flow field at time T=0. Both the recirculation zones are clearly visible. Subsequently, downstream vortex reduces in size while the upstream vortex increases. In Figure 4-19, the downstream vortex completely vanishes at t=T/2 and then reappears at t=T.

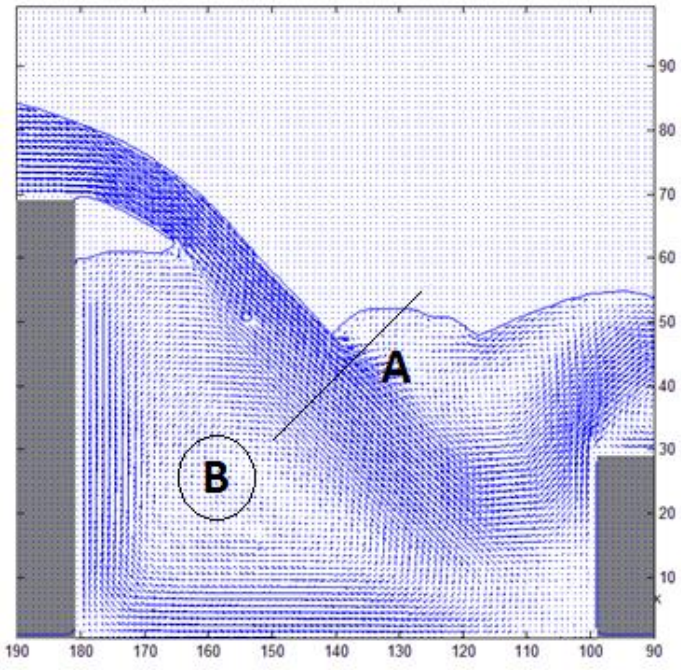

Figure 4-18 An Oscillatory Flow regime at t=0.

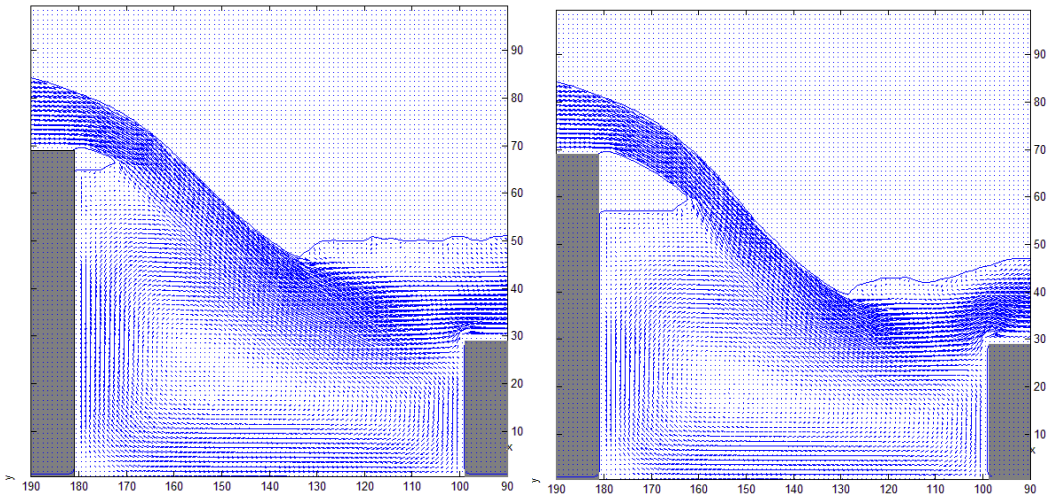

Figure 4-19 Flow fields throughout a period of T=1.8 s.

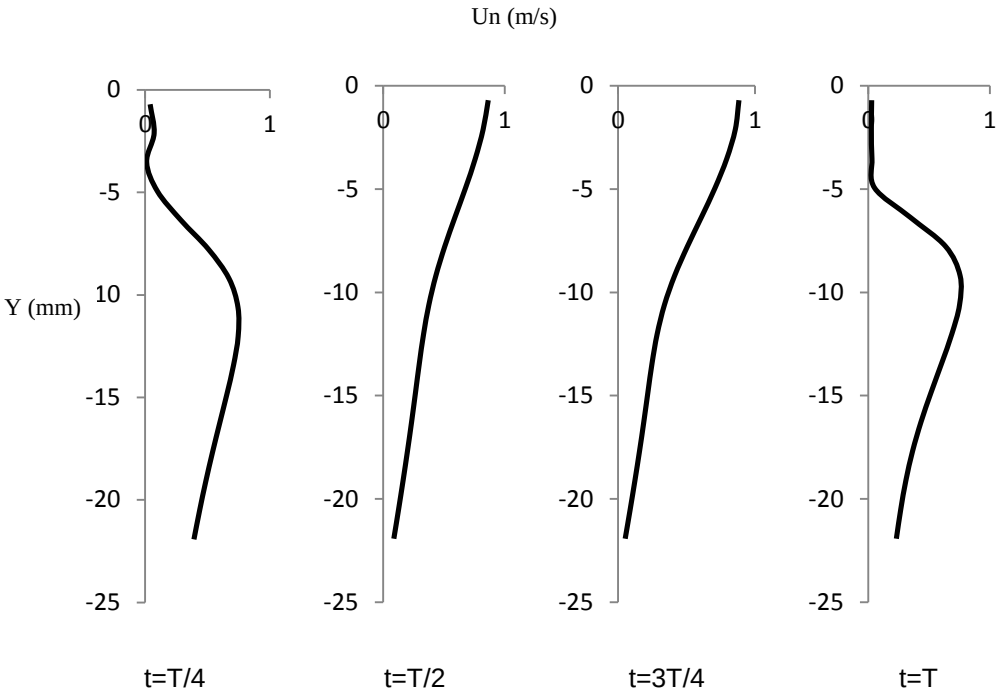

Figure 4-20 Velocities in shear layer at section A at different times (present study)

The velocity profiles in the shear layer are also shown in Figure 4-20. At t=T/2 and t=3T/4, the plots are similar to a typical velocity profile in shear layer when there is only one recirculation zone. The effect of another recirculation zone is evident from the top portion of the profile. At t= T/4, the velocity profile is distorted at the top which indicates the presence of a recirculation zone downstream. This is not the case for t=T/2 and 3T/4 which means that the vortex diminishes in size and eventually vanishes at some point of time. Towards the end of the cycle, the recirculation zone reappears and affects the shear layer.

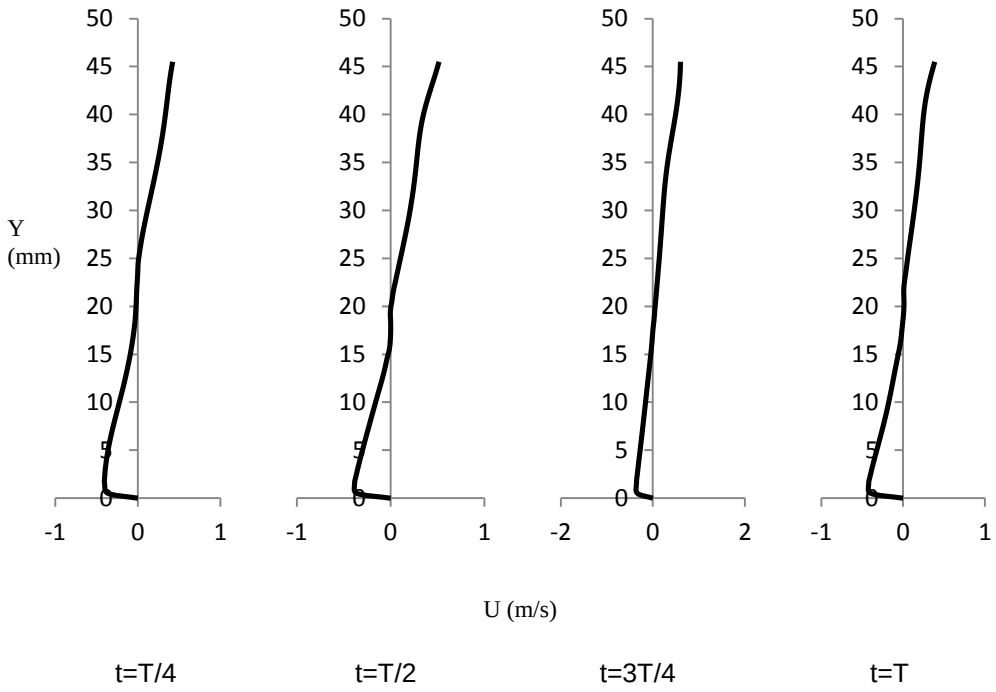

Figure 4-21 Velocities in recirculation zone located at B at different times (present study)

Horizontal velocity distribution in the recirculation zone which is below the incoming jet provides information about its location. As described earlier, the point where horizontal velocity changes direction marks the center of the recirculation zone. In Figure 4-21, the horizontal velocity in the recirculation zone is plotted against vertical distance from base. It is observed that the location of center of recirculation zone varies with time. At t=T/2, the center is at y=21.5 mm. At t=T/2 and 3T/4, it falls below this value. And by the end of cycle, it again increases. This indicates that the oscillatory effect is also observed in the location of the recirculation zone. The magnitude of velocity in this region indicates the strength of the vortex.

Chapter 5

Conclusion and Future Work

5.1 Conclusion

The study of flow field inside a vertically dropping pool is considered to be incompressible like all other open channel flows. The numerical solution of these problems involved solution of flow field using a finite volume scheme on a fixed uniform grid. One of the difficulties encountered in open channel flows is to find the location and orientation of free surface (interface). This was achieved using the coupled level set and volume of fluid method (CLSVOF) along with a piecewise linear interface construction (PLIC) scheme. The numerical code was executed for a wide range of parameters.

The study consisted of two parts. First is the study of flow field inside a vertically dropping pool without any obstacle or end sill. It was expected that there will be a skimming flow taking place inside the pool. Numerical simulations showed the same. There are two important regions in this type of flow: shear layer and recirculation zone. Hence the velocity distribution in these regions was closely examined and compared with experimental findings. The velocity profile in shear layer is quite different than that of a normal falling jet which can be explained by the fact that it interacts with the recirculation zone which creates the distortion. The nature of this profile is same throughout the shear layer unlike the cases with an obstacle. The velocities in the recirculation zone were also studied. This profile provides information about how deep the center of circulation is located. It is also seen that these profiles show a slight increase in velocity near the top which marks the beginning of shear layer. Thus it can be clearly observed that the shear layer and recirculation zone interact with each other and produce a typical skimming flow regime.

The second part of the study is about the flow field inside a vertically dropping pool with the presence of an obstacle or end sill. Unlike the previous case, there can exist three different flow regimes here: napped, periodically oscillatory and skimming. The study presented here shows all three flow regimes and the velocity distribution in the shear layer and recirculation zones. Napped flow occurs when the point of impingement lies inside the pool but closer to the base of fall. After impingement, one stream creates a recirculation zone underneath the incoming jet. The other stream encounters the obstacle in the path and thus generates an opposite circulating region downstream of the jet. Thus there are two recirculation zones which are opposite in nature and independent of each other. The shear layer is similar to a skimming flow only for a small distance. Most of the part of shear layer is affected by both the recirculation zones as shown in the results.

If the flow rate and velocity are sufficiently higher, then the point of impingement lies on the end sill rather than inside the pool. This means that the incoming jet effectively bypasses the pool and results into a skimming flow just as the first part of this study. The velocity profiles in shear layer and recirculation zones are also similar to respective profiles in the previous part. But there exists a small range of flow rate for which an intermediate flow regime occurs which is oscillatory in nature. This happens when the point of impingement is inside the pool but closer to the end sill. In this case, the velocity is not high enough for the end sill to be bypassed. But the two recirculation zones are not independent as well. Thus there exists an oscillatory behavior in the nature of these zones as explained earlier. Throughout one complete cycle, the shear layer resembles that of a skimming as well as a napped flow alternatively. The recirculation zone which is downstream of the incoming jet reduces in size, completely vanishes and again reappears towards the end of the cycle.

5.2 Future Work

This particular study is about the flow regimes based on the parameter (y/H) and indirectly the Froude number. Apart from this, the flow regimes also depend on the size of the pool. Hence the ratio of height of end sill to the height of fall (h/H) is another parameter which can have a significant impact on the type of flow. For this particular study this parameter was set to be equal to 0.43. A similar study can be done for different values of h/H ranging from 0 to 1. h/H = 0 corresponds to part one of this study which means that there is no end sill. Lower values of h/H will have a very small range of flow rates for which the flow is of napped regime and higher values of h/H will have a small range of flow rates for skimming regime.

The numerical solution for this study was done with the boundary conditions shown in chapter 3. It was mentioned that the obstacle has a rigid free slip condition. This means that the velocity at the wall of obstacle is not necessarily equal to zero. The boundary layer development will not happen in this case. Figure 5-1 (A) shows the velocity profile near the inlet region. The velocity of flow near the bottom (y=70 mm) is not zero. Figure 5-1 (B) shows a similar plot with experimental values. The velocity at the base (y = 11 cm) is actually zero. In all actual flows the boundary layer always develops from the base of the wall. But for open channel flows, this region is not significant. It does not affect the flow field in the pool and shear layer. Yet, it is advisable to incorporate this effect into the numerical solution to obtain even more accurate results.

Knowledge about the flow field opens the scope of research in application and development of newer technologies. Lin *et al*. proposed the idea of a Green Aerator [2] using the oscillatory behavior of flow inside the pool. Moreover, the knowledge about flow field in this region provides information about the energy dissipation occurring inside a vertically dropping pool which can be used to design efficient spillways.

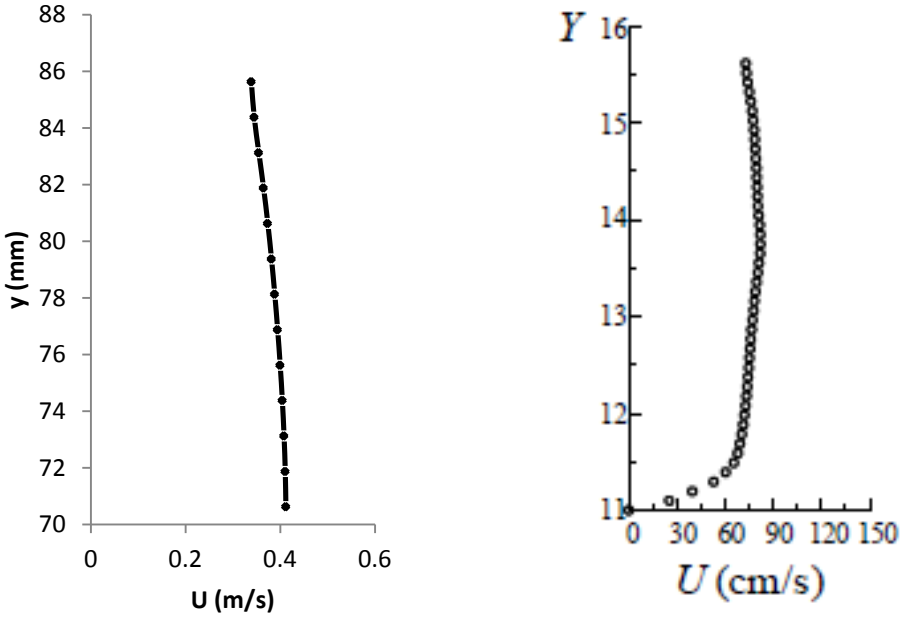

A B

Figure 5-1 Velocity profile near the inlet

(A) Numerical (B) Experimental

Appendix A

Code Execution

Execution of Code

The code used for this study is written in FORTRAN computer programming language. UNIX based high performance computing is used to compile and execute the program. The cases were run on two platforms.

- High Performance Computing at University of Texas at Arlington
- Lonestar system at Texas Advanced Computing Center, Austin

There are four basic files required to run the code.

- *bjob*
- *input*
- *filename.dat*
- *ripple*

All the files need to be placed under the same directory. *bjob* is the script file that provides load sharing facility instructions, generates a job id, places it in the appropriate queue and provides a destination path for the output files. *input* file has information about all the variables required by the program like fluid parameters, numerical parameters, boundary conditions etc. *filenam.dat* is a data file that has a list of names that serve as the file names for the output data files. *ripple* is the executable file that has algorithms needed for solving the problem.

Appendix B

Sample Input and Output

Sample Input File

One of the sample input files used for this study is shown here. It contains

```
#Flow over a vertically dropping pool
 $numparam
  alpha=2.0,
  conserve=.false.,
  autot=1.0,
  delt=1.0e-4,
  dtmax=1.0e-3,
  twfin=10000.0,
  con=0.3,
  fcvlim=0.5,
  idiv=1,
  dmpdt=3000000.0,
  prtdt=1000000.0,
  pltdt=5.0,
  sym=.true.,
  kt=6,
  kb=3,
  kl=2,
  kr=1,
 $end
 $fldparam
  gx=-9.8e-3,
  gy=0.0,
  icyl=0,
  isurf10=1,
  psat=0.0,
  xnu=7.3e-4,
  rhof=1.0,
  sigma=7.2e-2,
  vinf(2)=-0.355,
  vi=-0.355,
 $end
 $mesh
  nkx=1,
  xl=0.0,100.0,
  xc=50.0,
  nxl=50,
  nxr=50,
  dxmn=1.0,
  nky=1,
  yl=0.0,210.0,
  yc=105.0,
  nyl=105,
  nyr=105,
  dymn=1.0,
 $end
```

```
$obstcl
  nobs=4,
  oa1(1)=1.0, oc1(1)=-30.0, ioh(1)=1,
  ob1(2)=-1.0, oc1(2)=100.0, ioh(2)=0,
  ob1(3)=-1.0, oc1(3)=180.0, ioh(3)=1,
  oa1(4)=-1.0, oc1(4)=70.0, ioh(4)=0,
$end
$freesurf
  nfrsrf=4,iequib=0,
  fc1(1)=-1.0, ifh(1)=1,
  fa1(2)=1, fc1(2)=-87.0, ifh(2)=0,
  fa1(3)=1, fc1(3)=-70.0, ifh(3)=1,
  fb1(4)=1, fc1(4)=-200.0, ifh(4)=1,
$end
$graphics
  plots=.true., dump=.false.,
  iout = 0, 1, 0, 0, 0, 0, 0, 0, 0, 0, 0, 0, 0,
        0, 0, 0, 0, 0, 0, 0, 70, 88, 0, 0, 0, 0,
        0, 0, 0, 0, 0, 0, 0, 1, 0, 1, 1, 0, 1,
  iysymplt=0,
$end
$heateq
  heat= .false.,
  ischeme=3,
$end
$coupled
  lsvof=.true.,
  ls=.false.,
$end
```

Sample Output File

The output file generated during the simulation is named as *rippxxx.dat.* It contains the following information.

- Time at that instant
- Size of computational domain i.e. number of real cells in x and y direction
- Location of left side of cells in x direction and lower side of cell in y direction
- X and Y components of velocity
- VOF and LS Function values
- Enthalpy and Pressure

A sample out data file is shown below.

1.74000E+003	*Time*
2,100	*First real cell in X dir, last real cell in X dir*
2,210	*First real cell in Y dir, last real cell in Y dir*
0.00000E+000	*Location of left side of computational cell in X dir*
1.00000E+000	
2.00000E+000	
3.00000E+000	
…….	
0.00000E+000	*Location of lower side of computational cell in Y dir*
1.00000E+000	
2.00000E+000	
3.00000E+000	
…….	

0.00000E+000	0.00000E+000	1.00000E+000	-5.00000E-001	0.00000E+000	0.00000E+000
0.00000E+000	0.00000E+000	1.00000E+000	-5.00000E-001	0.00000E+000	0.00000E+000
0.00000E+000	0.00000E+000	0.00000E+000	5.00000E-001	0.00000E+000	0.00000E+000
0.00000E+000	0.00000E+000	0.00000E+000	1.50000E+000	0.00000E+000	0.00000E+000
Velocity comp in X dir	*Velocity comp in Y dir*	*VOF Function*	*LS Function*	*Enthalpy*	*Pressure*

References

[1] Lin C., Hwung W.-Y., Hsieh S.-C. and Chang K.-A., “Experimental study on mean velocity characteristics of flow over vertical drop”, Journal of Hydraulic Research”, Vol. 46, No. 3, pp. 424-428, 2008.

[2] Lin C., Hsieh S.C., Lo L.F., Chang S.Y. and Yang J (2012), “Green Aerator Using Periodically Oscillatory Flow Generated inside a Vertically Dropping Pool”. Paper presented at The 23rd International Symposium on Transport Phenomenon, Auckland, New Zealand.

[3] Lin W., Lin C., Hsieh S.C., Li C. and Raikar R.V, “Characteristics of Shear Layer Structure in Skimming Flow over a Vertical Drop Pool”, Journal of Engineering Mechanics, Vol 135, pp. 1452-1466, 2009.

[4] Lin C. Hsieh S.C., Lin W., Chou S.H. and Raikar R.V., “Flow Field in a Skimming Flow Over a Vertical Drop without End-Sill”, Journal of Mechanics, Vol. 115, pp. 1-20, 2012.

[5] Moore W. L., “Energy Loss at the Base of Free Over fall”, Trans. ASCE, Vol. 108, pp. 1343-1360.

[6] Chamani M.R. and Rajaratnam N., “Characteristics of Skimming Flow Over Stepped Spillways”, Journal of Hydraulic Engineering, Vol. 125, No. 4, pp. 361-368, 1999.

[7] Chamani M.R. and Rajaratnam N., “Jet Flow on Stepped Spillways”, Journal of Hydraulic Engineering, Vol. 120, pp. 254-259, 1994.

[8] Chanson H., Yasuda Y. and Ohtsu I., “Flow resistance in skimming flows in stepped spillways and its modeling”, Canadian Journal of Civil Engineering, Vol. 29, pp. 809-819, 2002.

[9] Chanson H., “Hydraulics of skimming flows over stepped channels and spillways”, Journal of Hydraulics Research, Vol. 32, No.3, pp. 445-460.

[10] Chow V.T., “Open Channel Hydraulics”, The McGraw-Hill Book Companies, Singapore, 1973.

[11] Kothe, D. B., Mjolsness, R. C., and Torrey, M. D., “RIPPLE: A computer program for incompressible flows with free surfaces”, Technical Report, LA-12007-MS, Los Alamos National Laboratory, 1991.

[12] Wang, Z., "Numerical Study on Capillarity- Dominant Free Surface and Interfacial Flows", Ph.D. Dissertation, Department of Mechanical Engineering, The University of Texas at Arlington, TX, 2006.

[13] Tong A.Y. and Wang Z., “A numerical method for capillarity-dominant free surface flows”, Journal of Computational Physics, Vol. 221, pp. 506-523, 2007.

[14] Wang Z. and Tong A.Y., “A sharp surface tension modeling method for two-phase incompressible interfacial flows”, International Journal for Numerical Methods in Fluids, Vol. 64, pp. 709-732, 2010.

[15] Kershaw, D.S., “The Incomplete Cholesky-Conjugate Gradient Method for the Iterative Solution of Systems of Linear Equations”, Journal of Computational Physics, Vol. 26, pp. 43-65, 1978.

[16] Shyy W., Udaykumar H.S., Rao M.M., and Smith R.W., “Computational Fluid Dynamics with Moving Boundaries”, Taylor and Francis, 1996.

[17] Harlow F. H. and Welch J. E., “Numerical calculation of time–dependent viscous incompressible flow of fluid with a free surface”, Physics of Fluids, Vol. 8, pp. 2182–2189, 1965.

[18] Hirt, C. W. and Nichols, B. D., “Volume of Fluid (VOF) Method for the Dynamics of Free Boundaries,” Journal of Computational Physics, Vol. 39, pp. 201-225, 1981.

[19] Sethian J. A., “Level set methods: Evolving interfaces in geometry, fluid mechanics, computer vision and material science”, Cambridge University Press, 1996.

[20] Osher S. J. and Fedkiw R. P., “Level set methods and dynamic implicit surfaces”, Springer–Verlag, New York, Inc., 2003.

[21] Sussman, M. and Fatemi, E., “An efficient interface-preserving level set redistancing algorithm and its application to interfacial incompressible fluid flow”, SIAM J. Sci. Comput., vol.20, No. 4, pp. 1165-1191, 1999.

[22] Son, G. and Hur, N., “A coupled level set and volume-of-fluid method for the buoyancy-driven motion of fluid particles”, Numerical Heat Transfer, part B, Vol.42, pp. 523-542, 2002.

[23] Rudman, M., “Volume-Tracking Methods for Interfacial Flow Calculations,” International Journal for Numerical Methods in Fluids, Vol. 24, pp. 671-691, 1997.

Biographical Information

Vimal Ramanuj was born in Riyadh, Saudi Arabia and brought up in India. He aspires to become a professor and a researcher in the field of Fluid and Thermal Science and the use of Numerical Techniques in this area. He attended Nirma University in India where he received his B. Tech in Mechanical Engineering. His work in undergraduate studies was concentrated in Heat Exchangers, Solar Thermal Conversion and Computational Techniques in Fluid Dynamics. He then entered The University of Texas at Arlington for M.S. in Mechanical Engineering and joined Dr. Tong's research group to work on Numerical Techniques in Fluid Flows. After completing his M.S., he wishes to continue for the Ph.D. program at UT Arlington and further his research.